

High-resolution temperature profiling in the LACIS-T wind tunnel and the Pi Chamber

by Robert Grosz

contact: rgrosz@fuw.edu.pl



Motivation

- thermal characterization of both facilities;
- Improve strategies for future experiments, instrumentation positioning;
- only a comprehensive understanding of full spectrum of scales analyses can effectively link together different phenomena;

Ultrafast Thermometer (UFT)



UFT-2A (left) and UFT-2B (right)

- 1992 – prototype, $\sim 50 \mu\text{m}$ thick thermocouple
- 1997 – UFT, resistive platinum-coated tungsten wire, $2.5 \mu\text{m}$ thick, 5 mm long, $\sim 50 \Omega$ resistance, and time constant $\sim 10^{-4}$ s

UFT-M (POST, 2007), UFT-2-0 (ACORES, 2017),
UFT-2A and UFT-2B (EUREC⁴A, 2020)

The current versions of UFT, UFT-2A and UFT-2B,
utilize 3 mm long wire spanned on an industry
miniature wire probes by DANTEC®

Haman, K. E., *et al.*, (1997), Kumala, W., *et al.*, (2013)

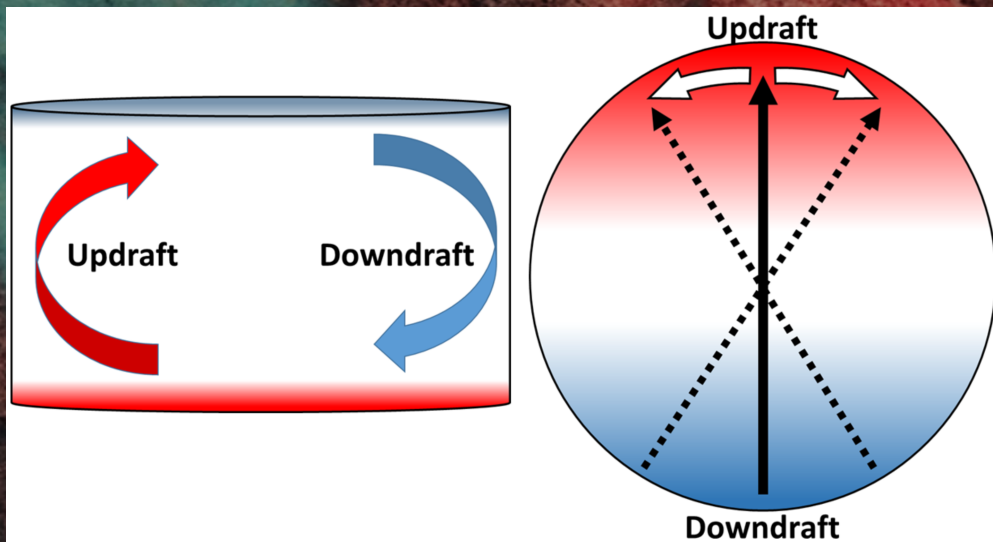
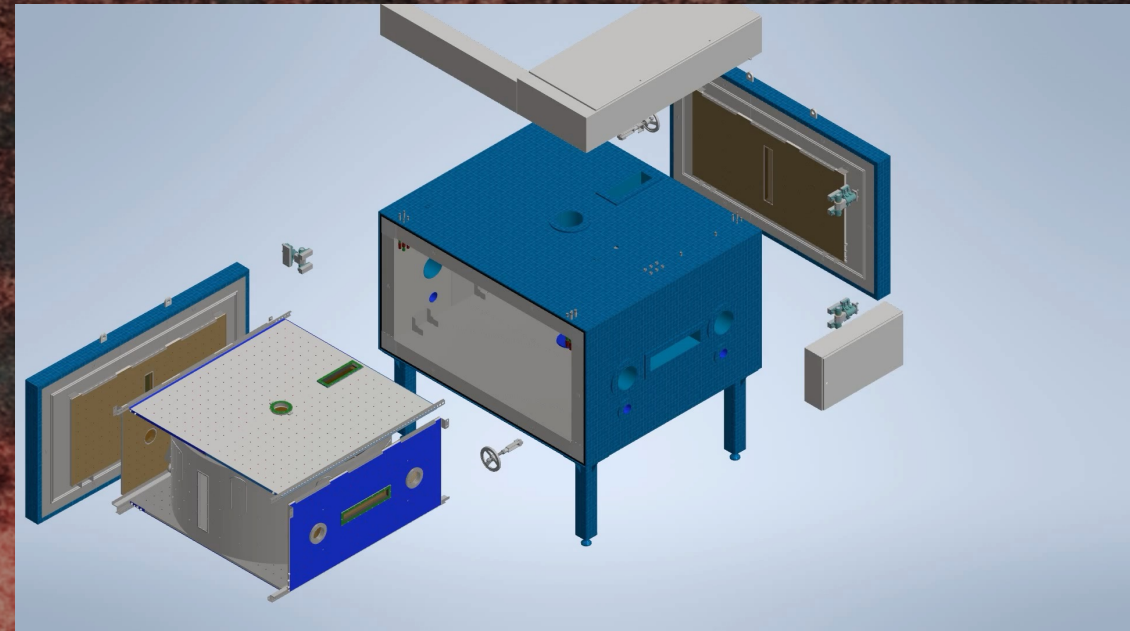


Part I
the Pi Chamber

Setup

- reproducible and controlled measurements across a wide range of temporal scales (minutes to days)
- operates in two modes (pressure reduction and Rayleigh-Bénard convection)

Chang, K., *et al.*, (2016)

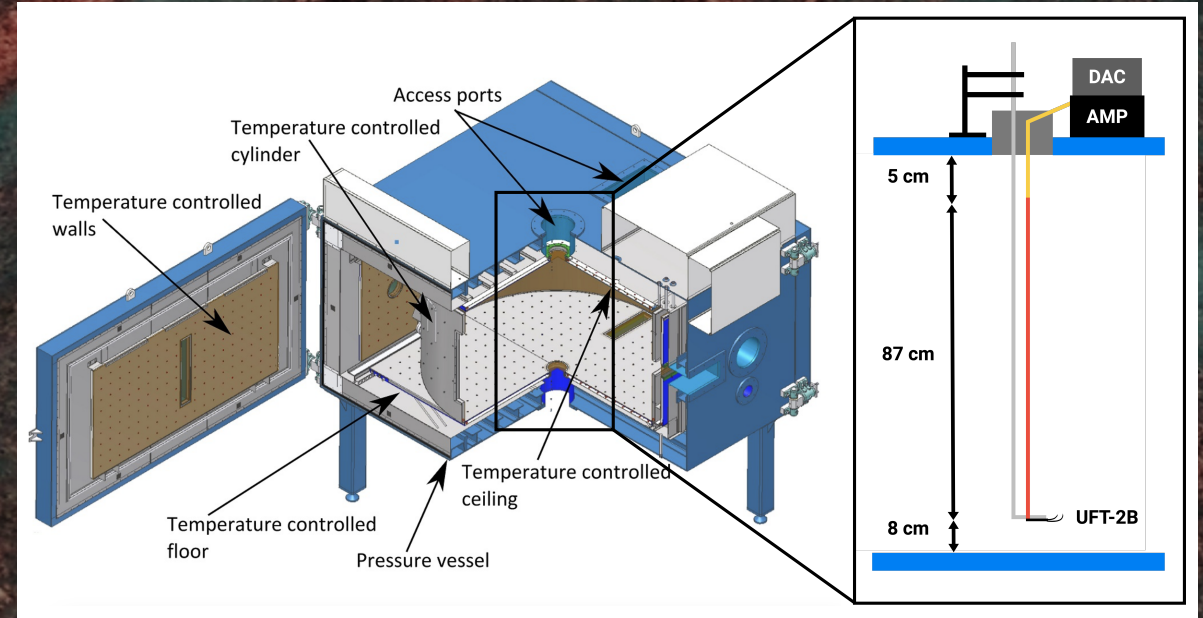


- The established large-scale circulation (LSC) period (single roll) for temperature difference $\Delta T = 12$ K, was approximated to $\tau_{12} \approx 72$ s (moist convection with mixing ratio of 7.55 g kg^{-1}).

Anderson, J. C., *et al.*, (2021)

Strategy

- high resolution (2 kHz) temperature time series at selected locations in a vertical profile near the axis of the chamber
- investigation under three ΔT : 10 K, 15 K, and 20 K at Rayleigh number $Ra \sim 10^9$ and Prandtl number $Pr \approx 0.7$



- variable measurement time (3 min or 19 min)
- less emphasized aspect—the surface topography, i.e. longitudinal stripes on the floor and ceiling (aluminum bars, 4 cm wide and 1.4 cm high, separated by 17 cm intervals)

Experiment	Boundaries type	ΔT [K]	h [cm]	t [min]	Ra [$\times 10^9$]
V10-S-L	smooth	10	irregular	19	1.1
V10-S	smooth	10	8–95	3	1.1
V15-S-L	smooth	15	irregular	19	1.6
V15-S	smooth	15	8–95	3	1.6
V20-S-L	smooth	20	irregular	19	2.1
V20-S	smooth	20	8–95	3	2.1
V20-R	rough	20	8–95	3	2.1

The irregular positions are: 8, 14, 26, 35, 50, 65, 74, 86, 95 [cm].

Strategy

Experiments' name explanation:

V20-S-L

V – vertical profiling

20 – ΔT

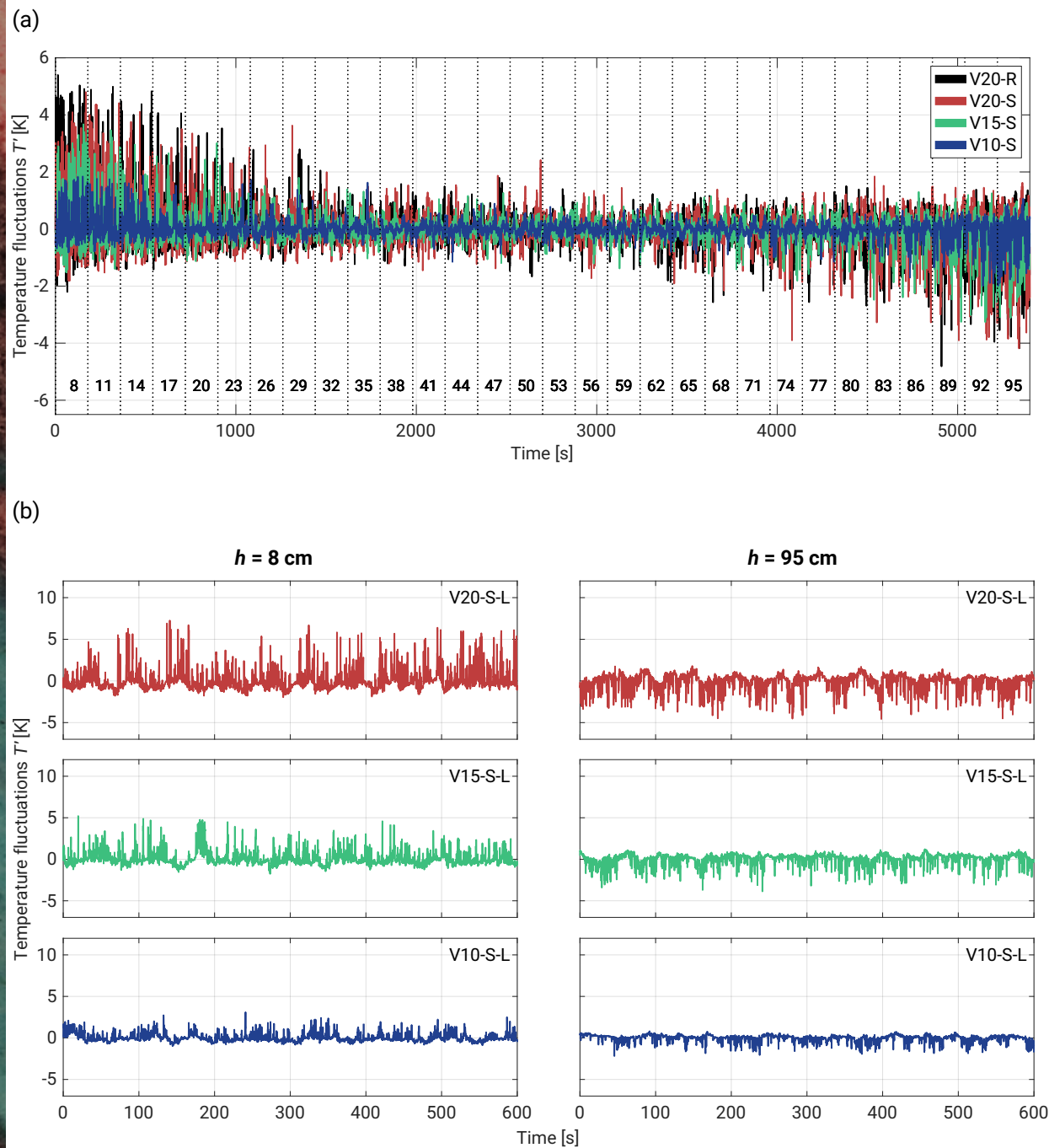
S – type of boundaries (S for smooth and R for rough)

L – 19 min measurement time

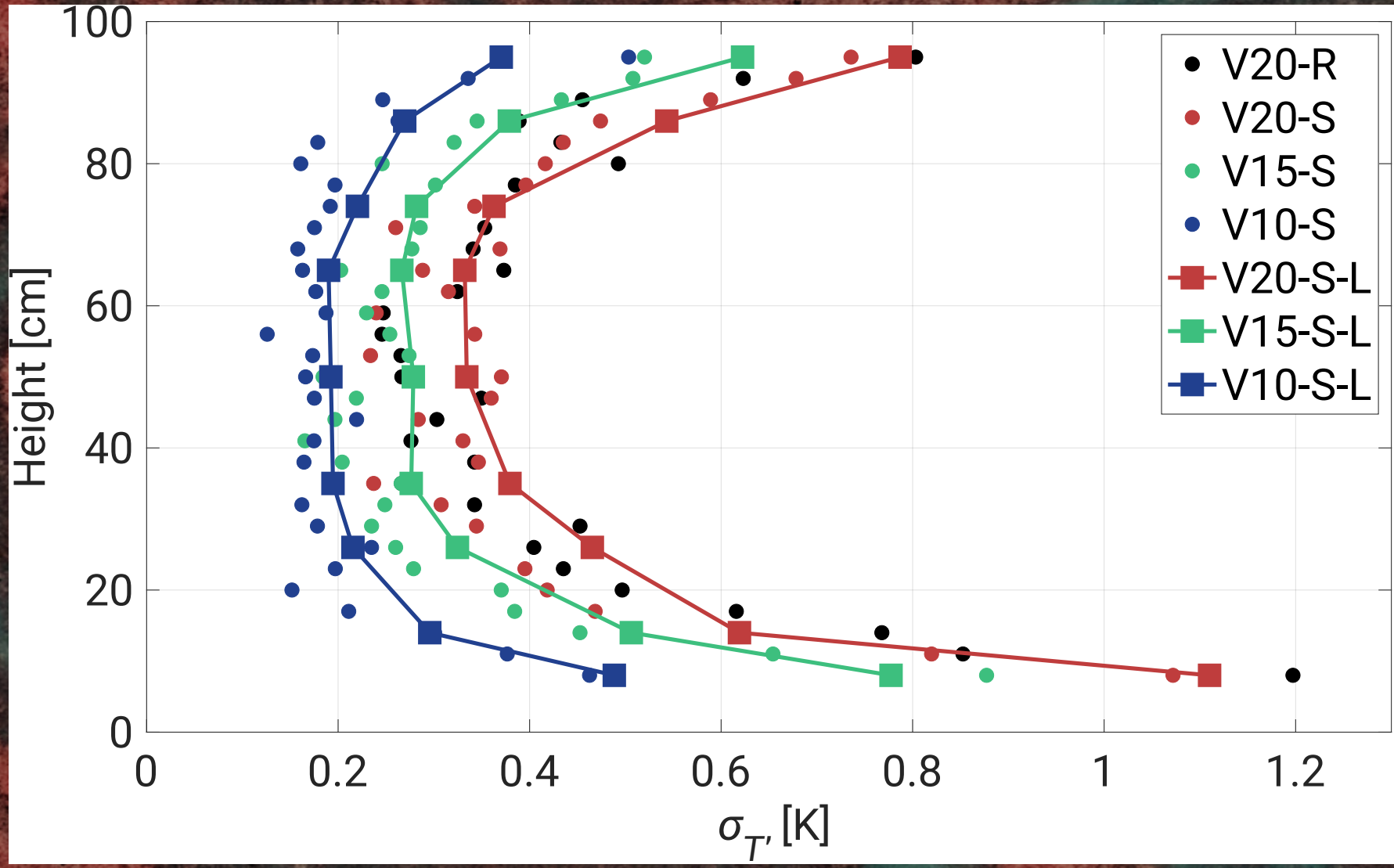
Experiment	Boundaries type	ΔT [K]	h [cm]	t [min]	Ra [$\times 10^9$]
V10-S-L	smooth	10	irregular	19	1.1
V10-S	smooth	10	8–95	3	1.1
V15-S-L	smooth	15	irregular	19	1.6
V15-S	smooth	15	8–95	3	1.6
V20-S-L	smooth	20	irregular	19	2.1
V20-S	smooth	20	8–95	3	2.1
V20-R	rough	20	8–95	3	2.1

The irregular positions are: 8, 14, 26, 35, 50, 65, 74, 86, 95 [cm].

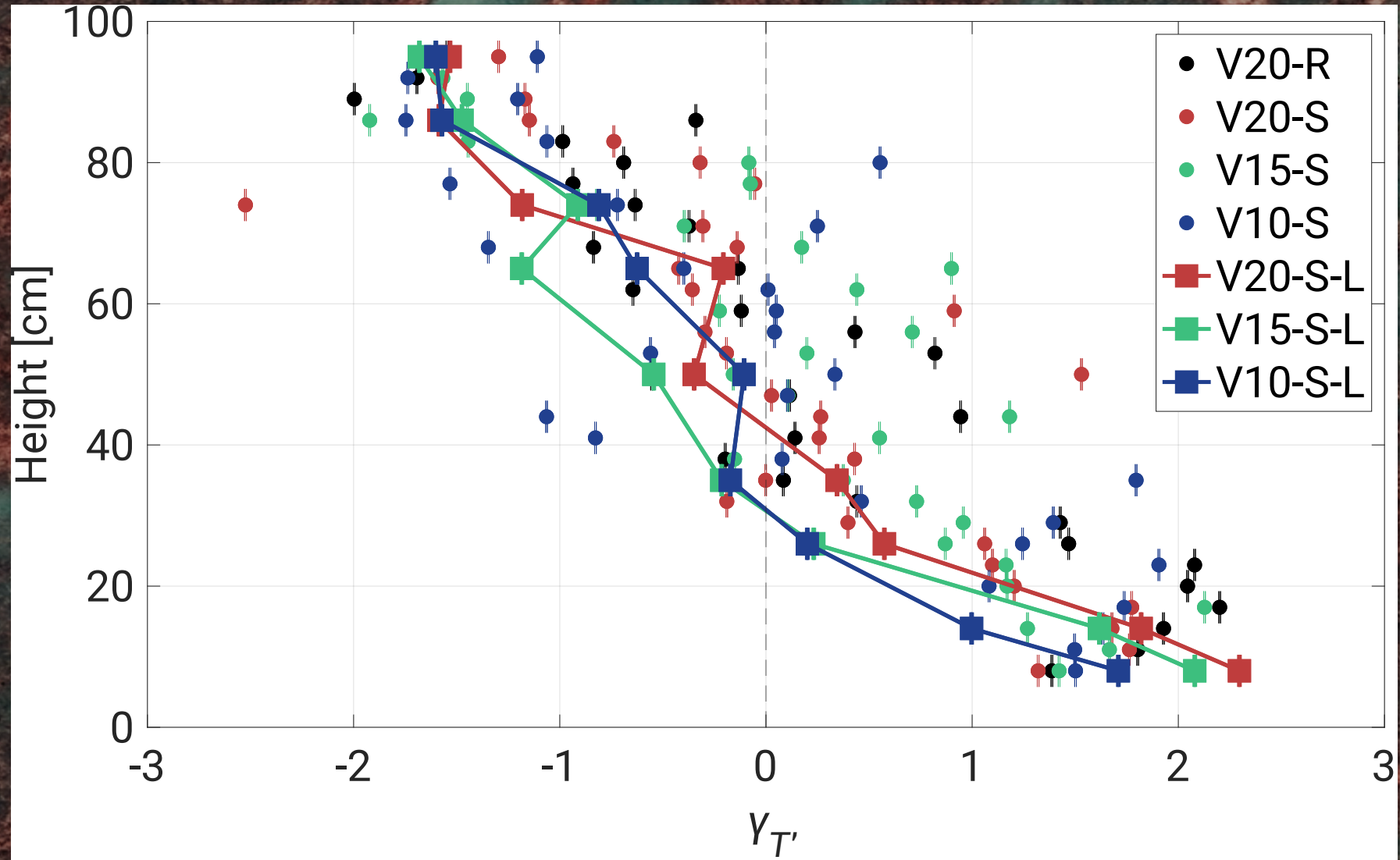
Results



Standard deviation

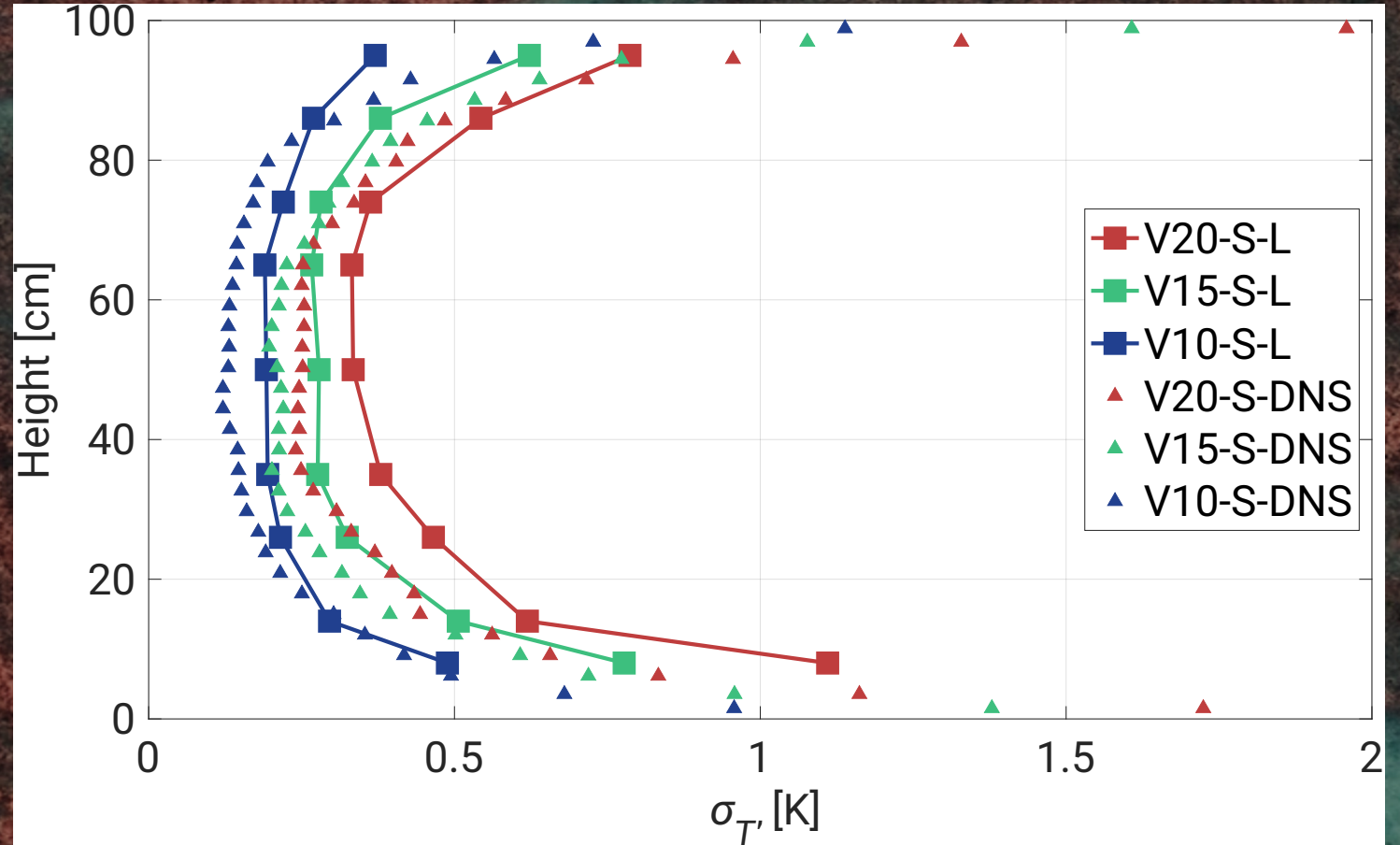


Skewness

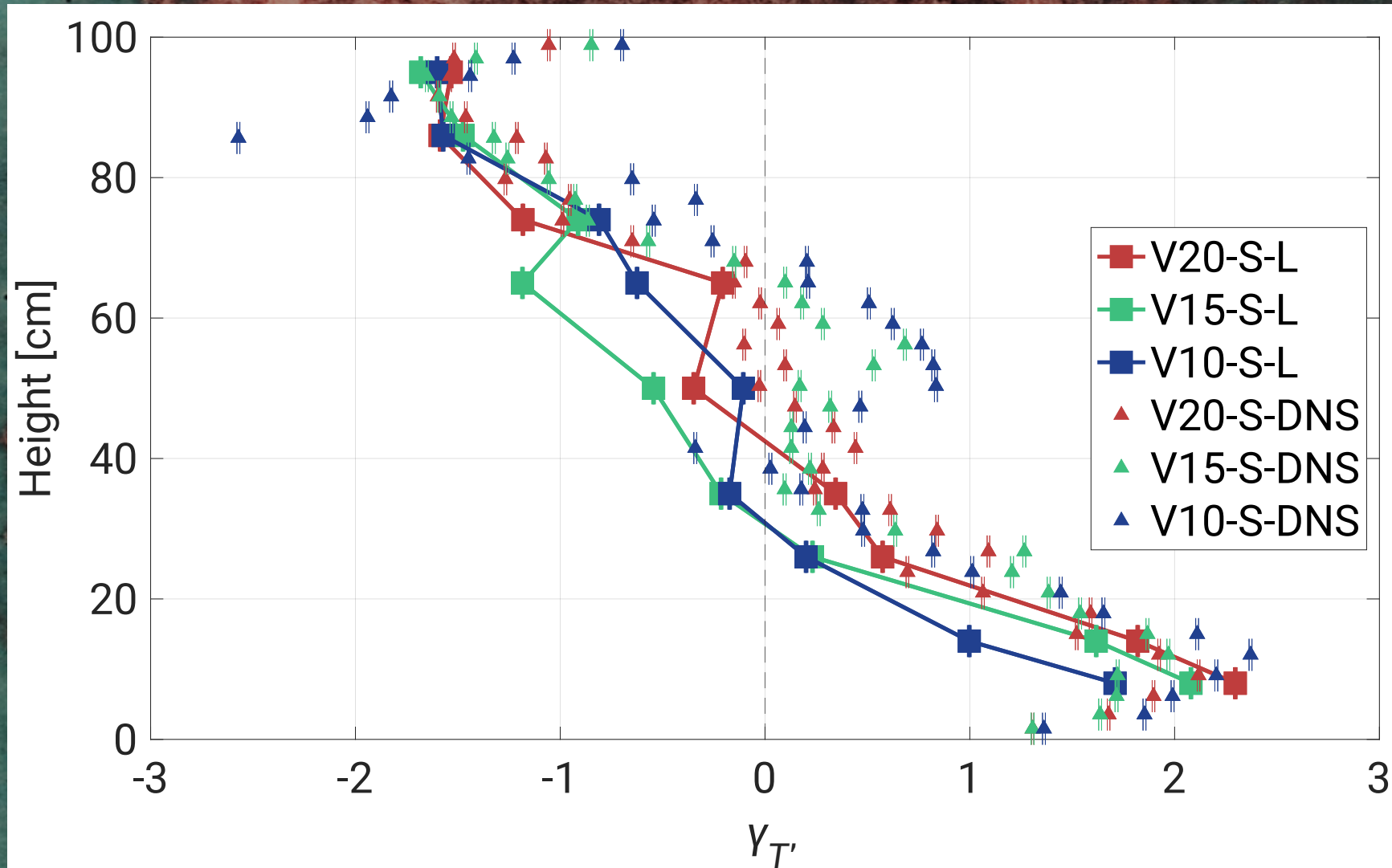


DNS vs experiment – standard deviation

- Cloud Model 1 (CM1) (Bryan and Fritsch, (2002)) with the computational domain size $960 \times 960 \times 500$ grid cells. The model and setup are described in detail in Chandrakar *et al.*, (2022, 2023)
- temperature boundary conditions are consistent with the experiments, the Eulerian temperature time series are outputted at 0.0012–0.0015 s

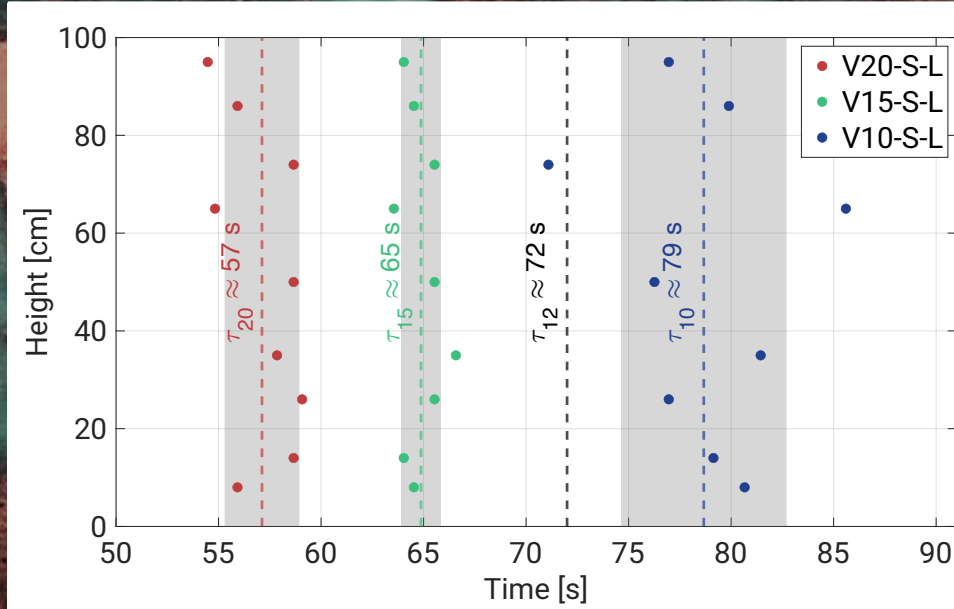


DNS vs experiment – skewness

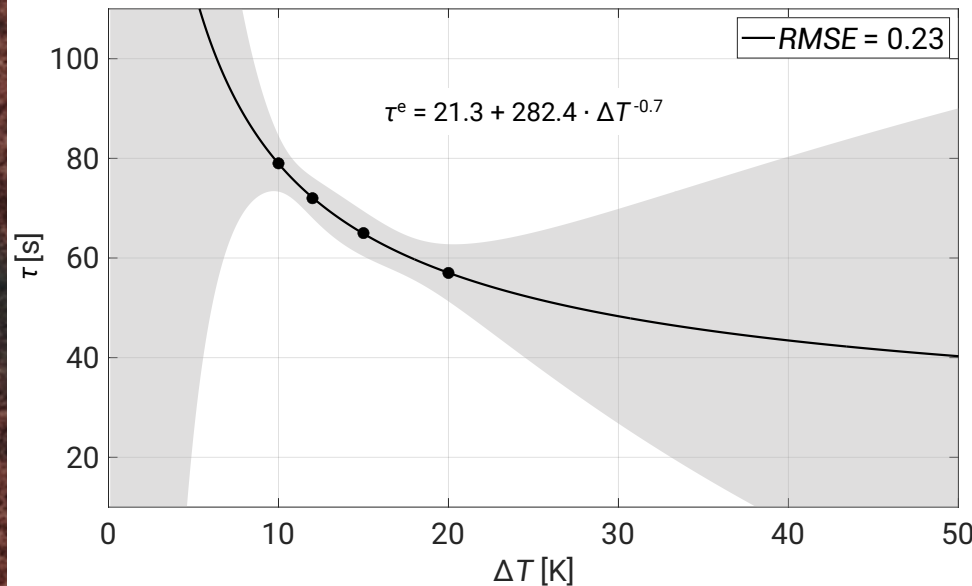


large-scale circulation

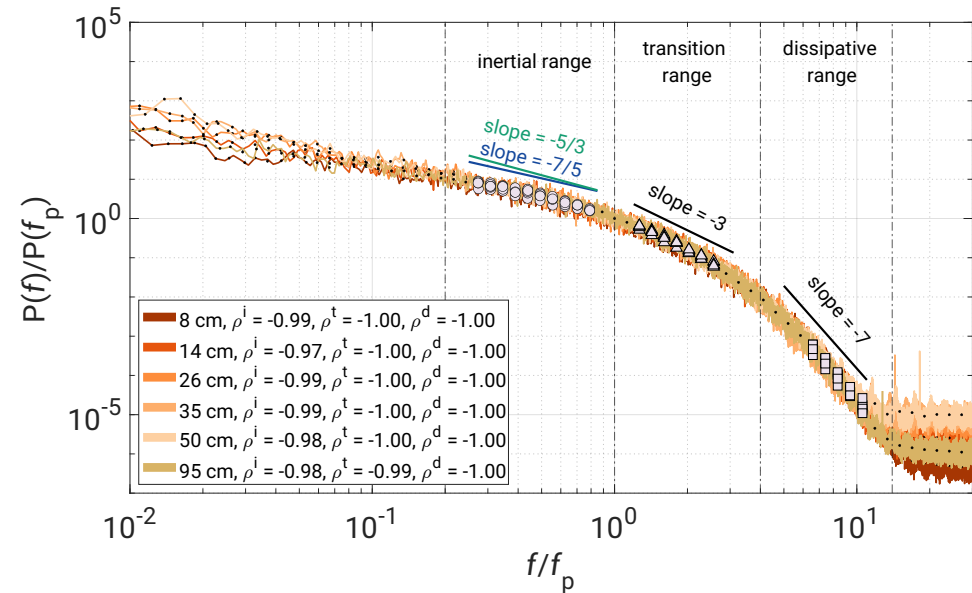
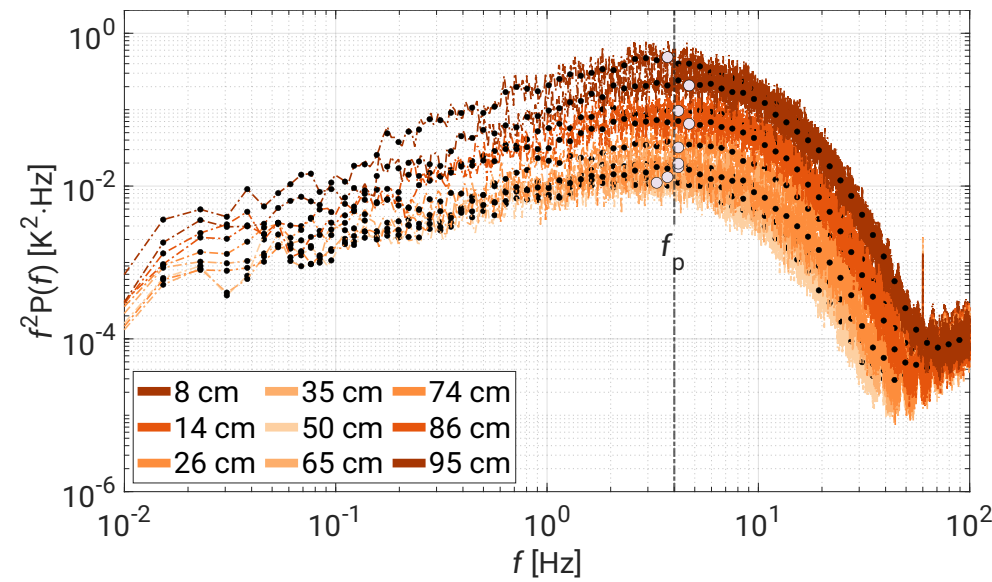
- relationship between τ and ΔT modeled by exponential function
- plot includes 95% simultaneous functional bounds, and root mean squared error (*RMSE*)



- vertical variability of the LSC period
- grey regions describe $\pm 1\sigma$
- $\tau_{12} \approx 72$ s obtained by Anderson *et al.* (2021) for $\Delta T = 12$ K



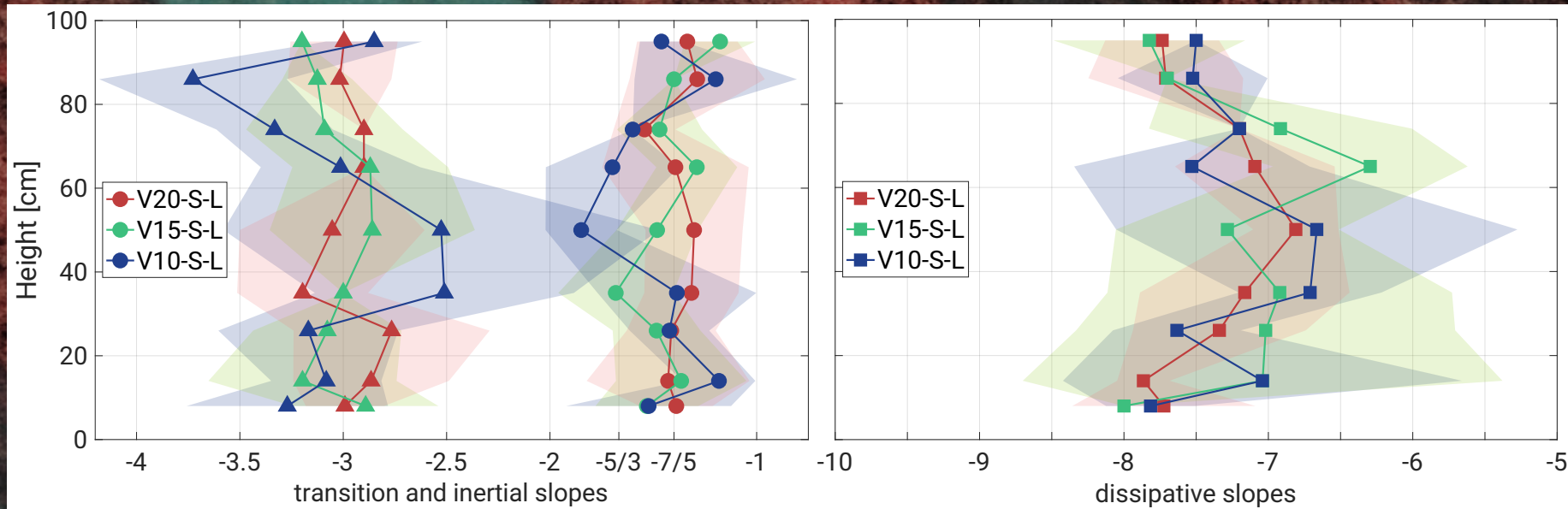
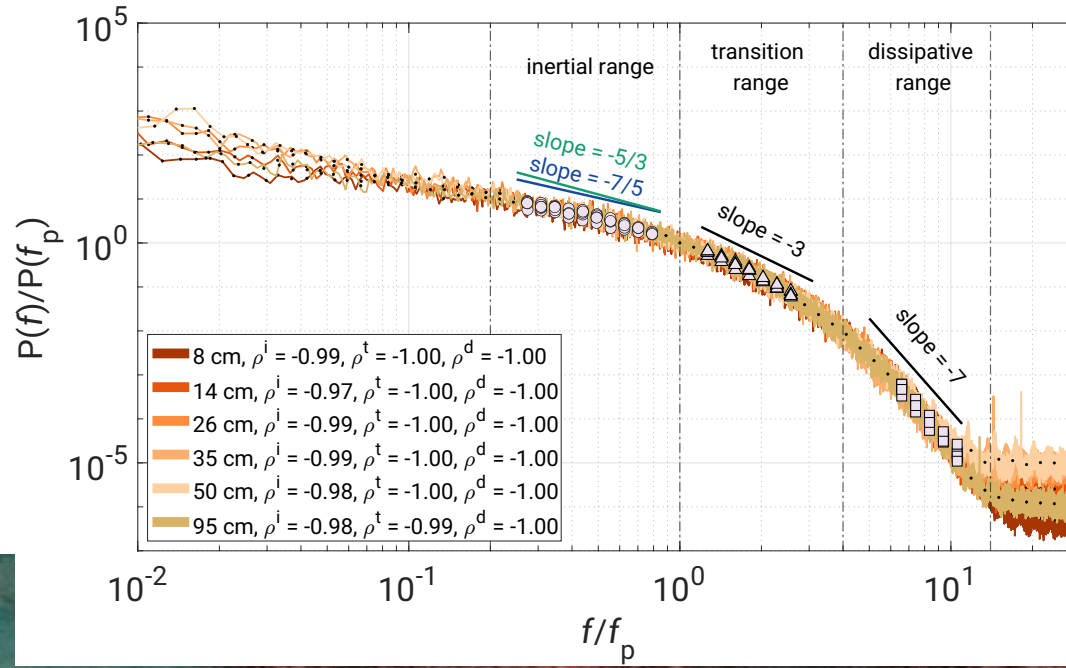
- scaling method proposed by Zhou and Xia (2001) – $f^2 P(f)$ – to collapse the PSD curves
- high convergence across all curves around $f_p = 4$ Hz



Power Spectral Density – collapse

- three spectrum regimes: inertial, transition, and dissipative
- linearity of the slopes in log-log coordinates estimated with the Pearson correlation coefficient ρ

Power Spectral Density – slopes



Passive scalar spectrum

- no direct references in the literature address the subsequent regime scalings (~ -3 and ~ -7) or the roll-off region of the scalar spectrum
- recent investigations of the dissipation range in the energy spectrum only began exploring this regime suggesting a superposition of two exponential forms (Khurshid *et al.*, 2018; Buaria and Sreenivasan, 2020).

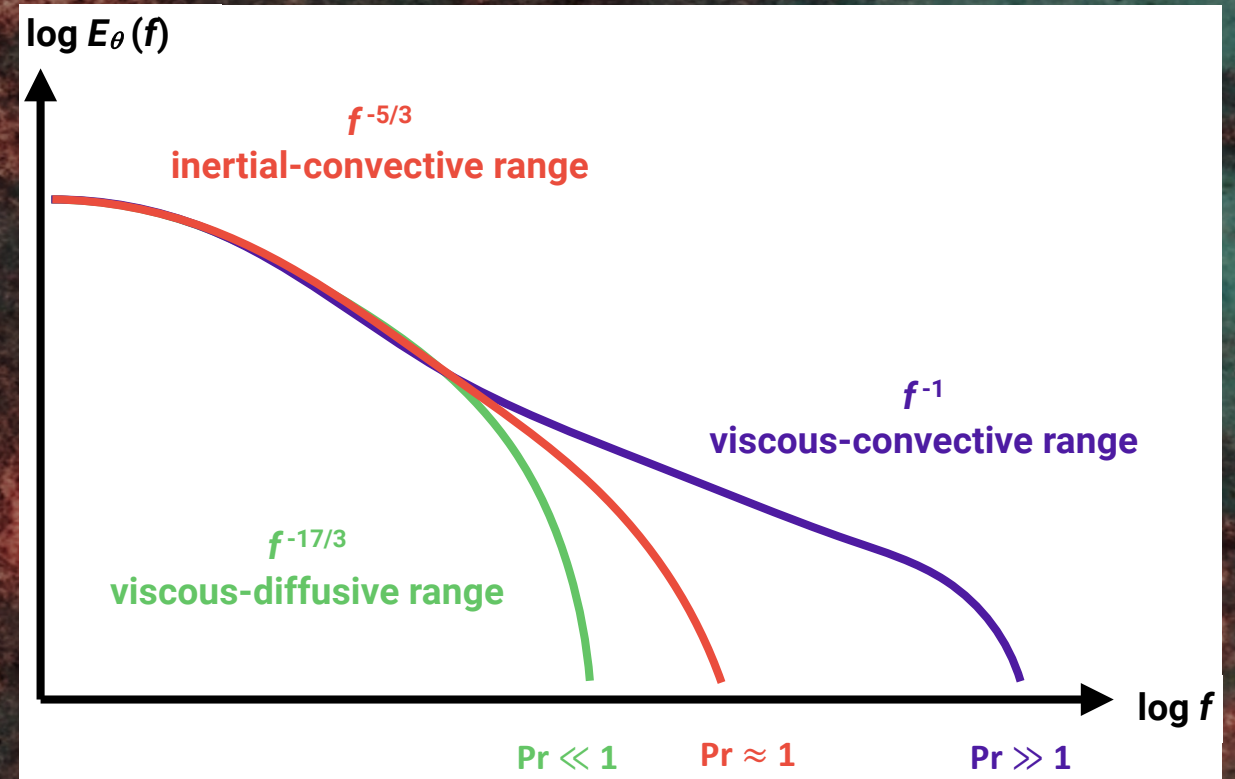
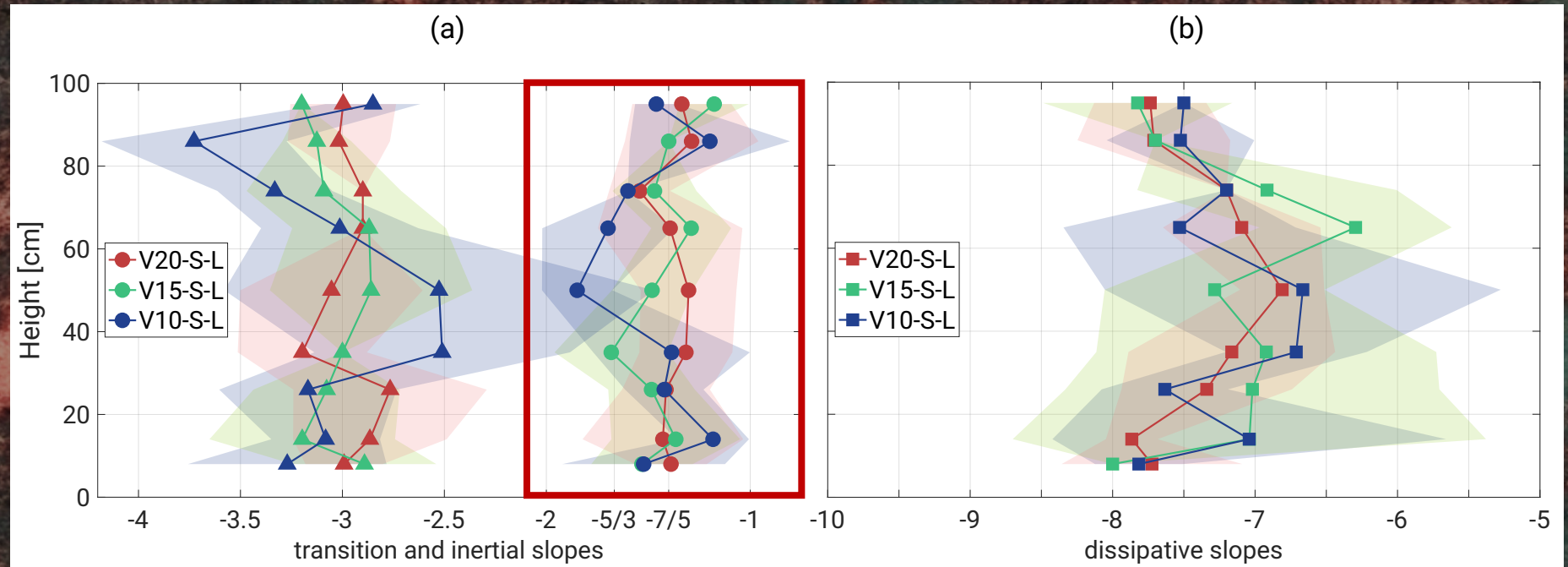


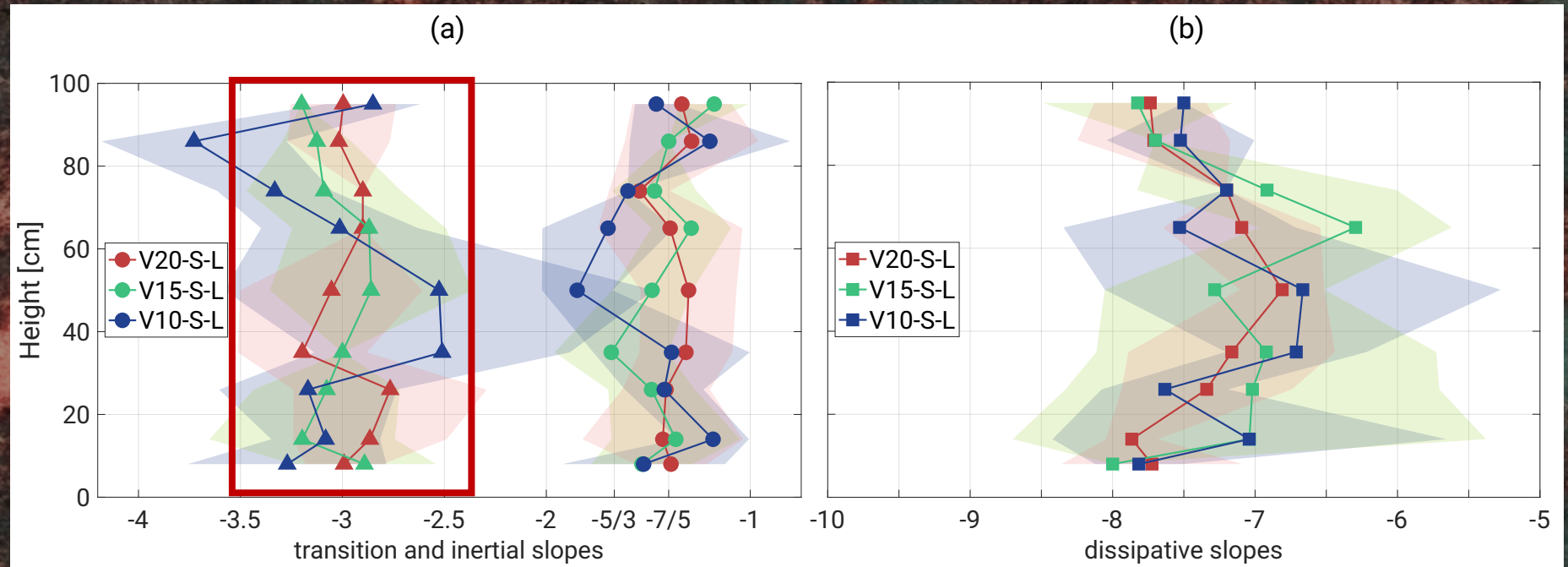
Figure adapted from Gotoh and Yeung (2012)

Power Spectral Density – slopes



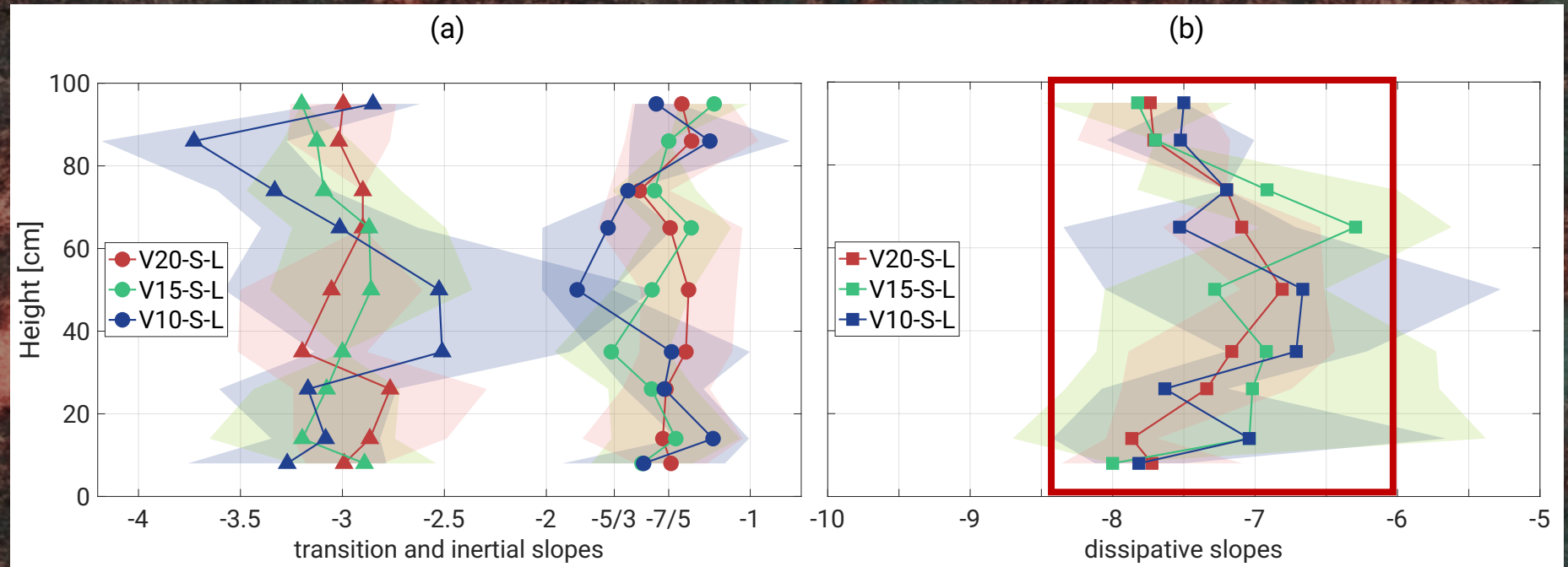
- inertial-convective regime is associated with Obukhov-Corrsin scaling ($-5/3$), where the temperature field does not influence the flow dynamics
- in thermally-driven convection, the flow is actively driven by temperature-induced buoyancy differences. This range is therefore redefined as the inertial-buoyancy range, where the temperature spectrum follows Bolgiano-Obukhov scaling ($-7/5$)

Power Spectral Density – slopes



- the -3 scaling might simply represent a crossover into the following dissipative range
- LES studies on thermal plumes (Chen and Bhaganagar, 2021, 2023, 2024):
 - density and temperature spectra scale as -2.7 , strongly correlated with the velocity spectrum
 - vertical heat and mass fluxes exhibited a -3 scaling, matching the vertical component of the turbulent kinetic energy (TKE) spectrum
 - both spectra of 2D TKE, horizontal structures of 3D TKE, as well as helicity, consistently exhibited slopes of $-5/3$ and -3 respectively

Power Spectral Density – slopes

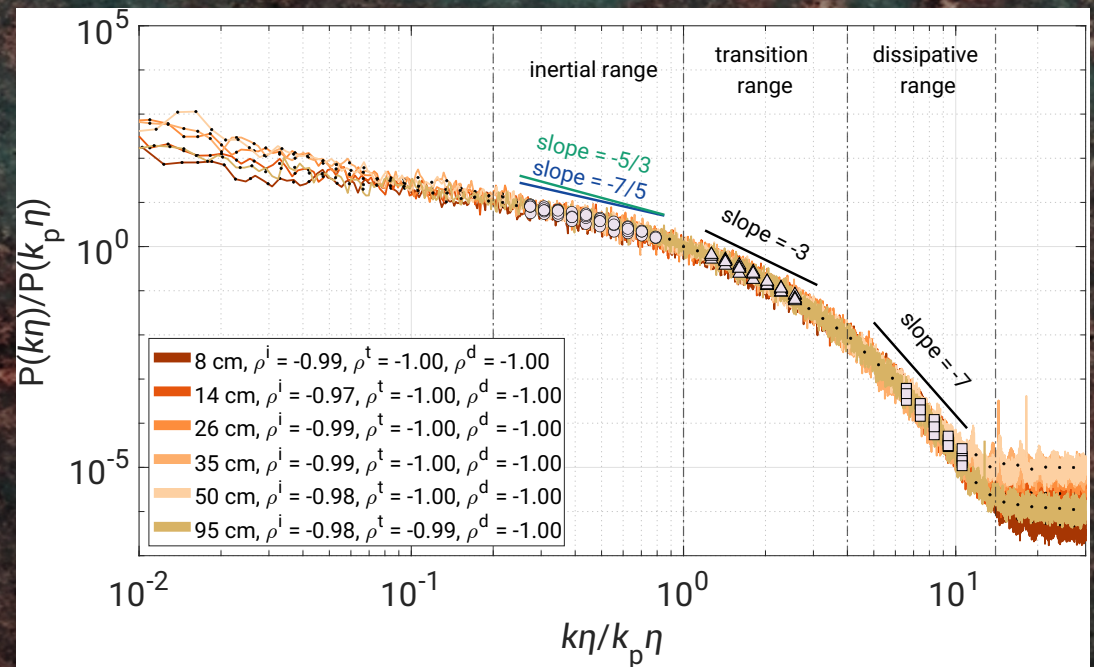
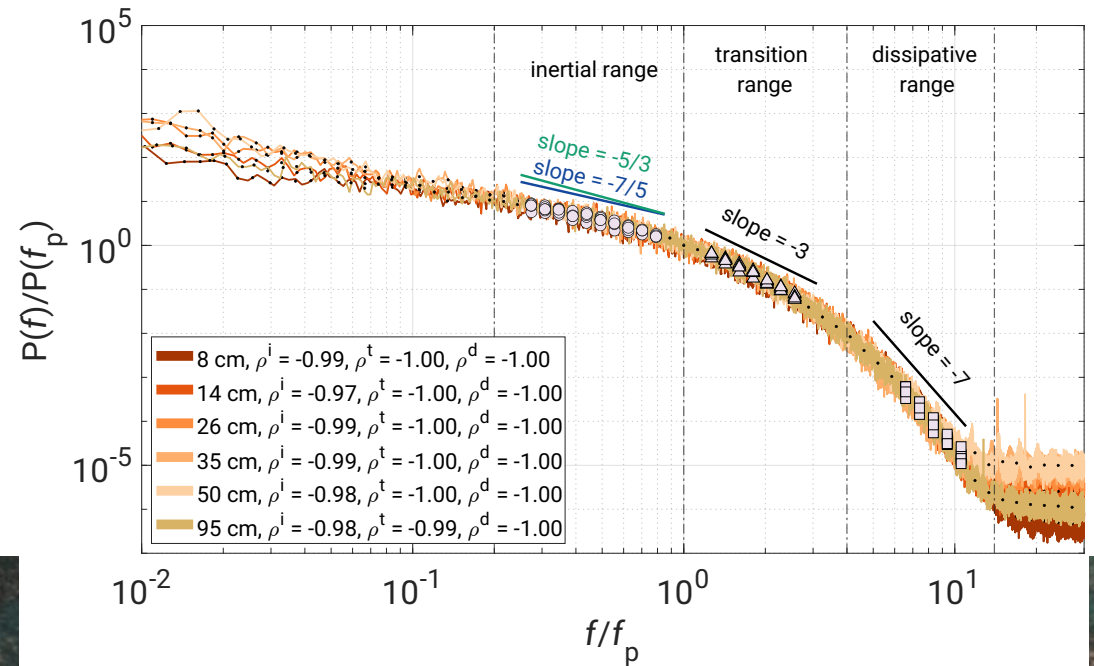


- according to Sreenivasan (2019), no scalar spectrum description exists for the dissipative regime
- in the given study a single power law seemed to be sufficient to describe this regime

Power Spectral Density in wavenumber picture

$$k \approx \tilde{f} = f(2\pi)U$$

$$P(k) \approx P(\tilde{f}) = P(f)U/2\pi$$



Power Spectral Density in wavenumber picture

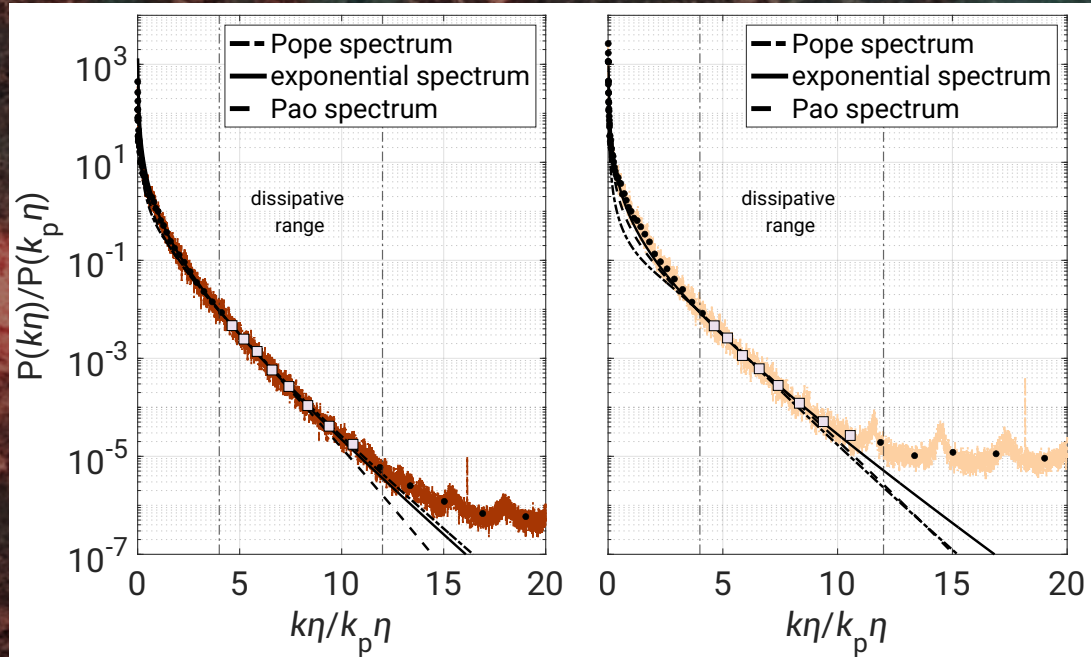
$$E(k) = C_K \langle \epsilon \rangle^{2/3} k^{-5/3} \underbrace{f_L(kL)}_{\approx 1} f_\eta(k\eta)$$

- Pope: $f_\eta(k\eta) = \exp\left(-\beta \left\{ [(k\eta)^4 + c_\eta^4]^{1/4} - c_\eta \right\}\right)$
- exponential: $f_\eta(k\eta) = \exp(-\beta k\eta)$
- Pao: $f_\eta(k\eta) = \exp(-\beta \{k\eta\}^{4/3})$

$$E_\theta(k) = C_\theta \langle \epsilon_\theta \rangle \langle \epsilon \rangle^{-1/3} k^{-5/3} f_\eta(k\eta)$$



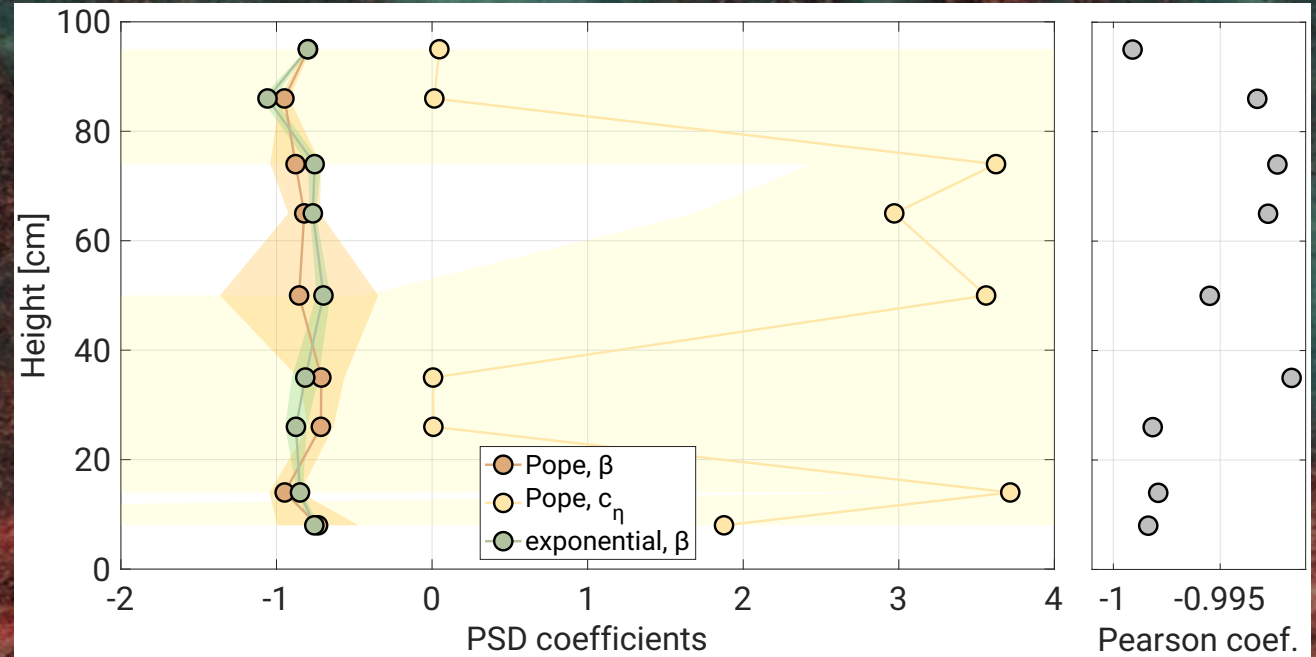
Power Spectral Density in wavenumber picture



$h = 8$ cm

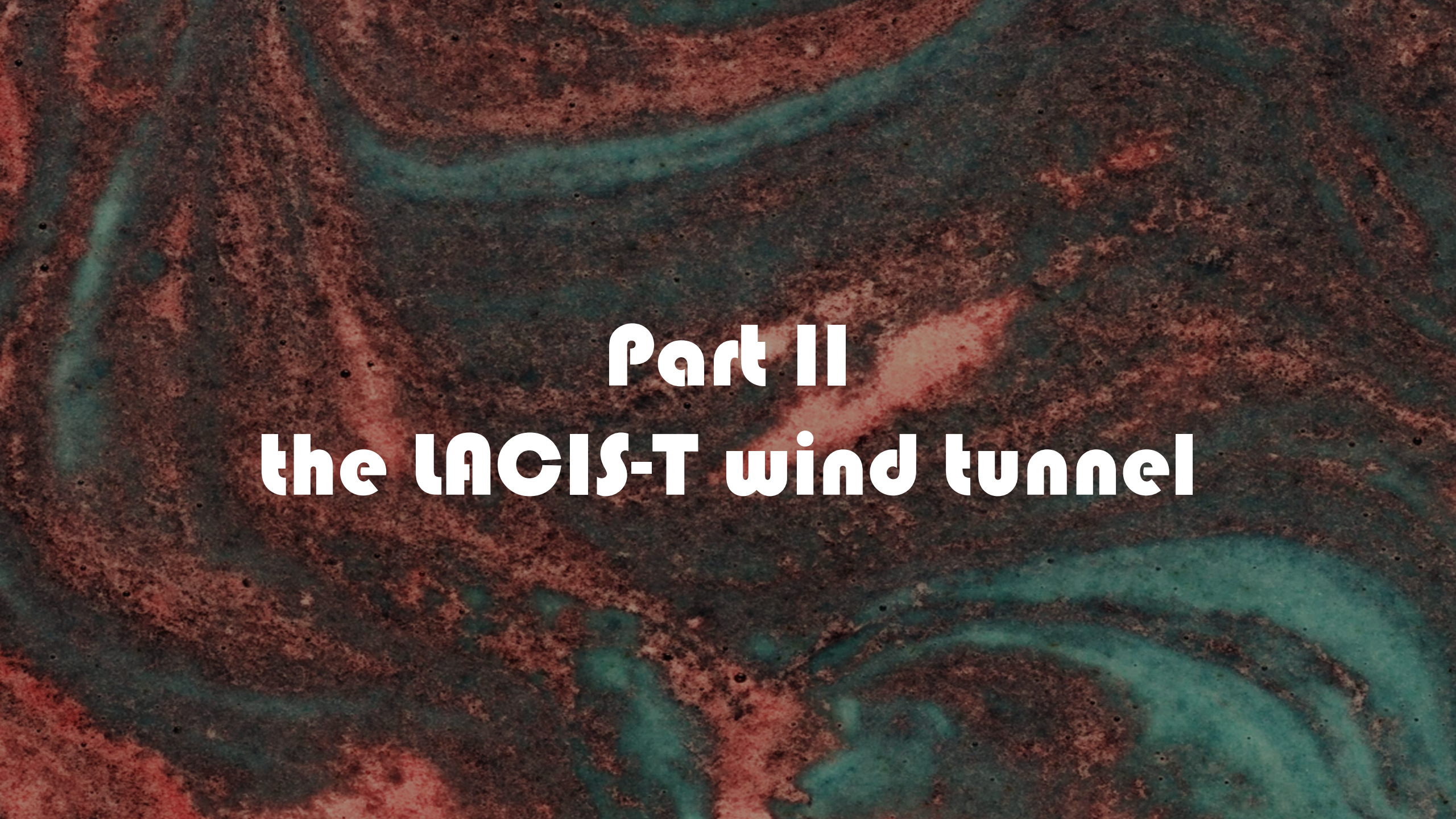
$h = 50$ cm

$\Delta T = 20$ K



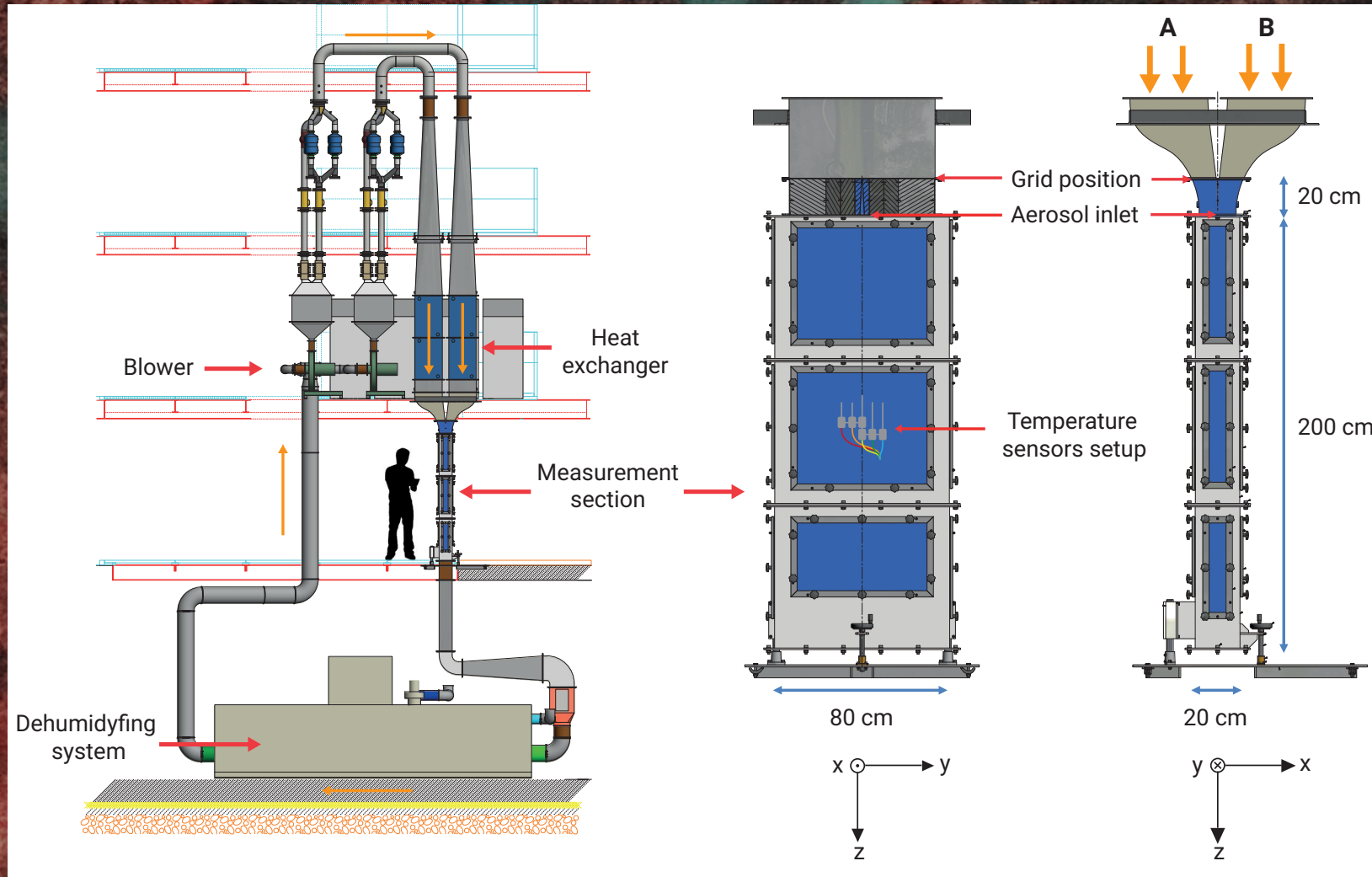
1 part-take away

- basic characteristics – significant changes in the standard deviation, skewness, and the scaling exponents of the power spectrum of the distribution of temperature fluctuations near the top and bottom surfaces -> dynamics of local thermal plumes and their interaction with the LSC
- topographic effects – no major differences were observed corresponding to topographic effects -> likely due to insufficient time series
- dynamic regimes – PSD analysis revealed periodicity of LSC with respect to the temperature differences; three distinct power-law dynamic regimes were identified: inertial ($\sim -7/5$), transition (~ -3), and dissipative (~ -7); the scale break between the inertial and transition ranges -> a dynamic transition from the LSC-dominated regime to the thermal plume regime; the following dissipative regime analyses confirmed usability of analytical approach for the scalar spectrum;
- experiment versus DNS – experimental findings showed convincing agreement with DNS conducted under similar thermodynamic conditions;
- please see Grosz R., *et al.*, (2024) for a broader discussion



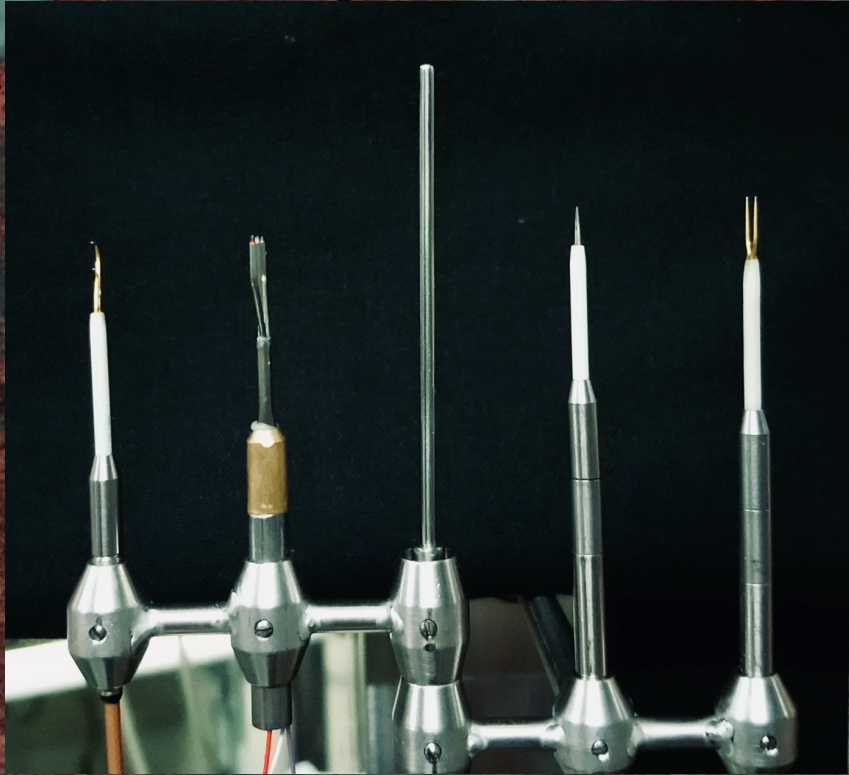
Part II
the LACIS-T wind tunnel

Setup



Niedermeier *et al.*, (2020), and Nowak *et al.*, (2022)

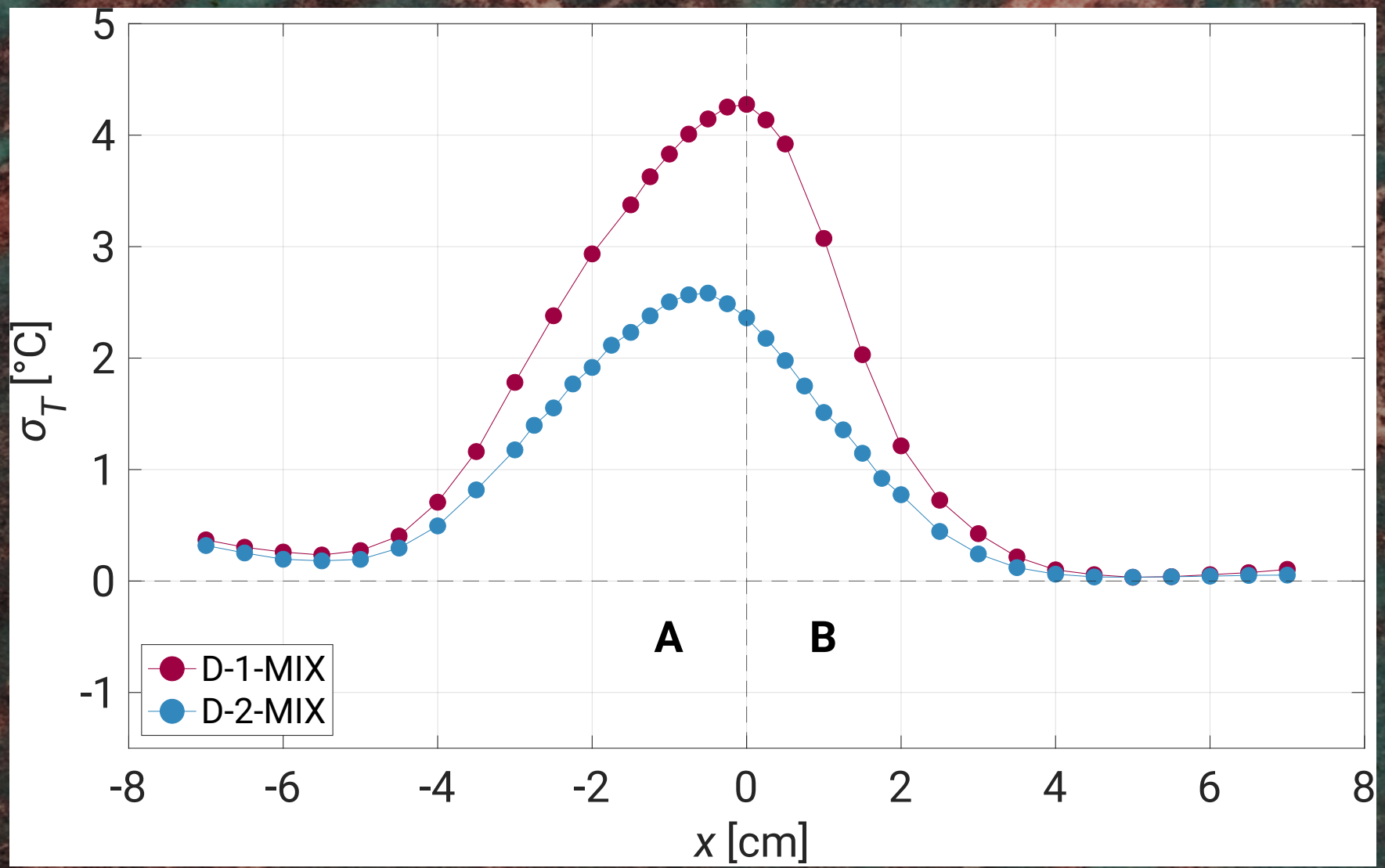
Strategy



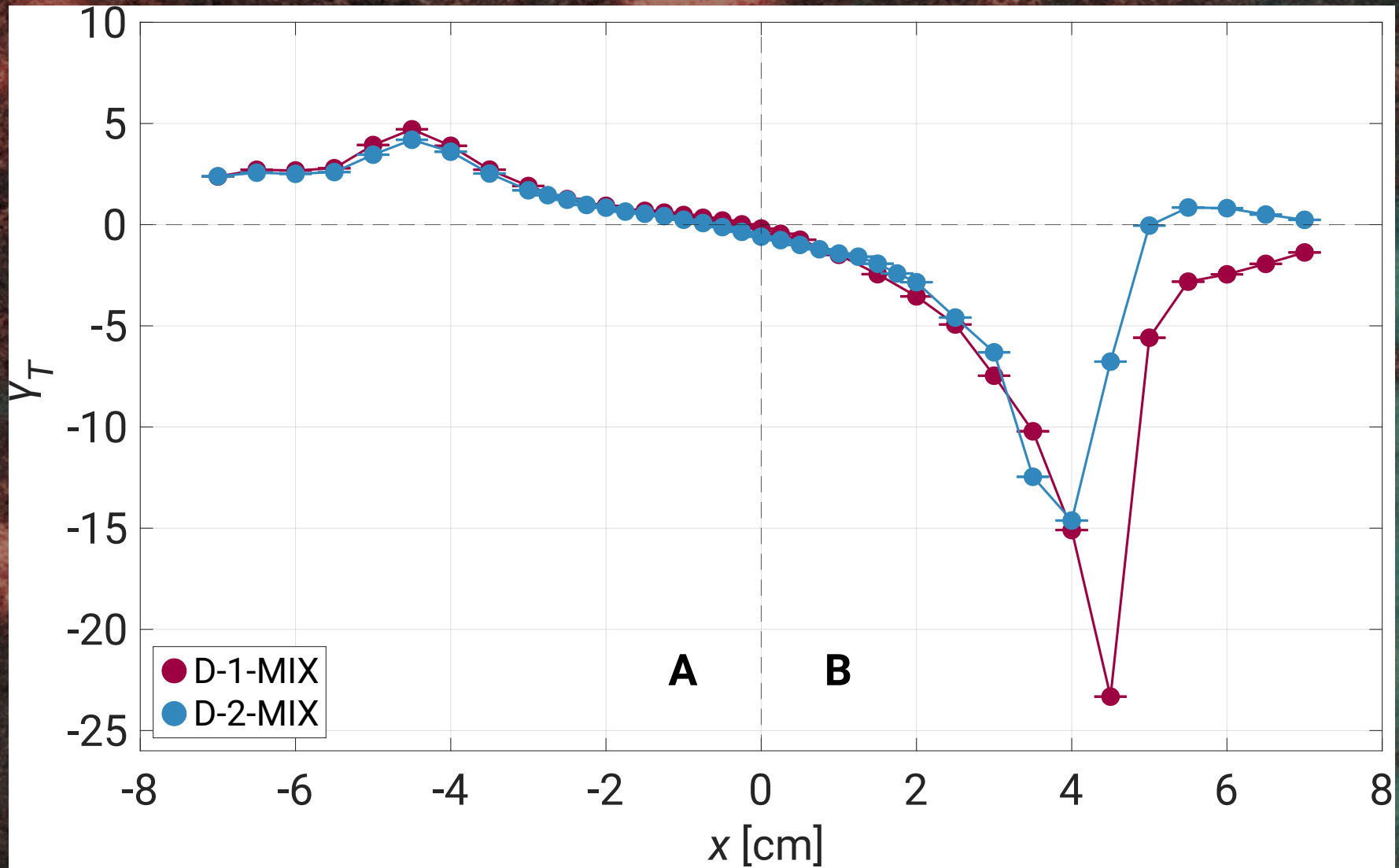
Experiment	T_A [°C]	F_A [m ³ min ⁻¹]	T_B [°C]	F_B [m ³ min ⁻¹]	x [cm]	t [min]
D-1-MIX	0	6.1	25	4.5	-7 to 7	10
D-2-MIX	4	4.5	20	4.5	-7 to 7	5

- high resolution (1.5 kHz) temperature time series along the x axis
- study performer under two ΔT : 25 K, and 16 K
- variable measurement time (10 min or 5 min)
- note different flow rates between both streams in D-1-MIX

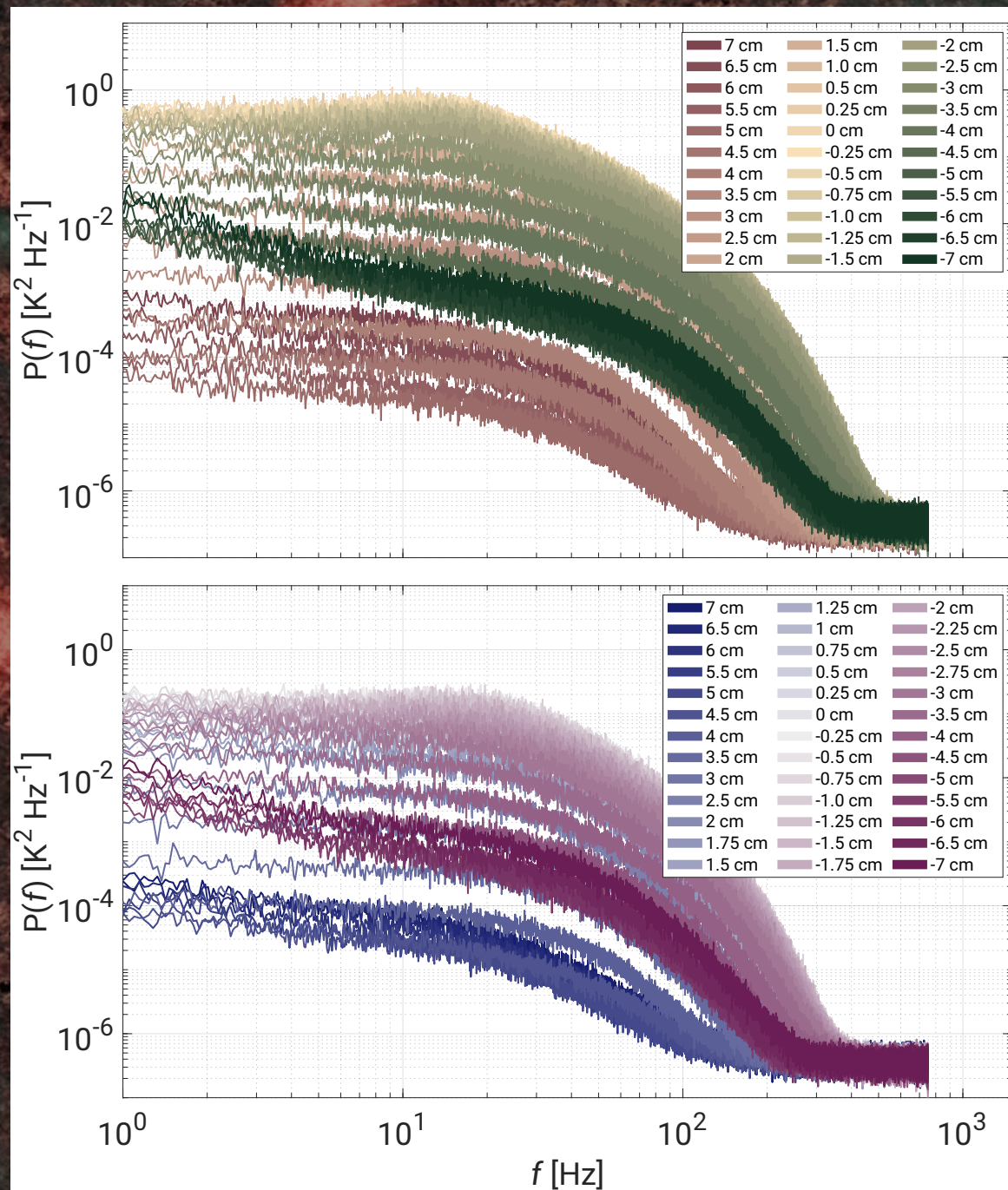
Standard deviation



Skewness



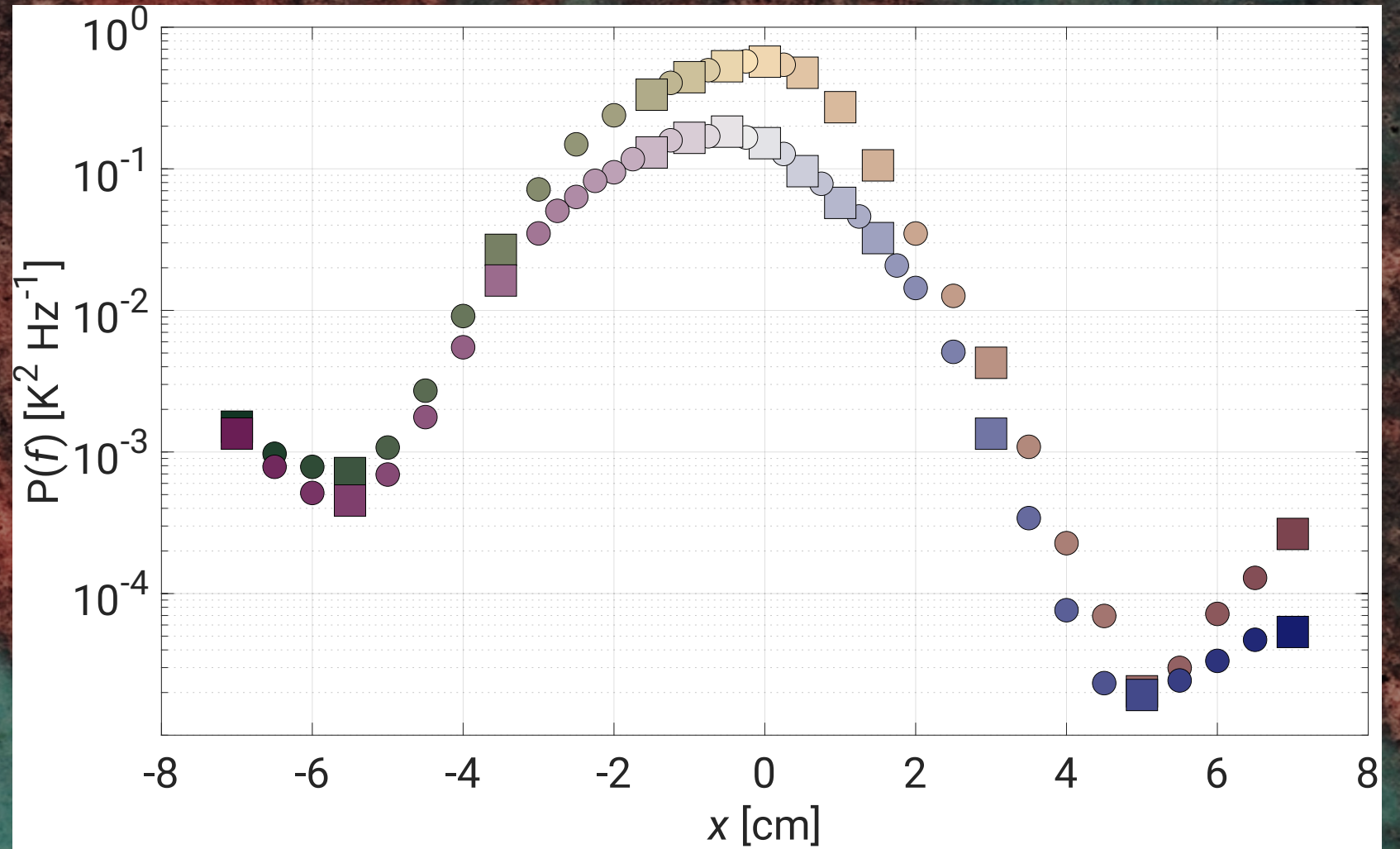
Power Spectral Density - raw



D-1-MIX

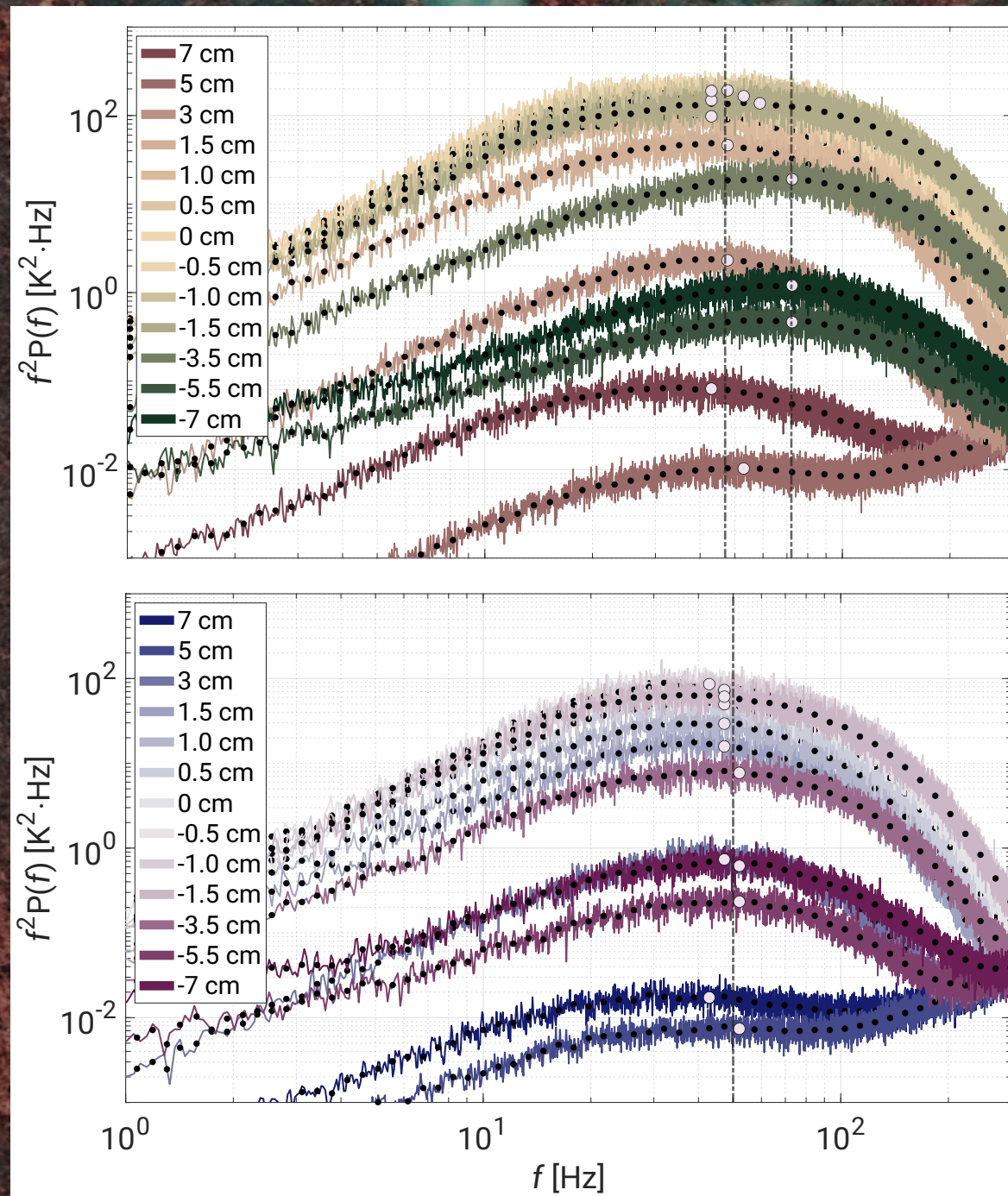
D-2-MIX

Power Spectral Density – cross-section



Power Spectral Density – collapse

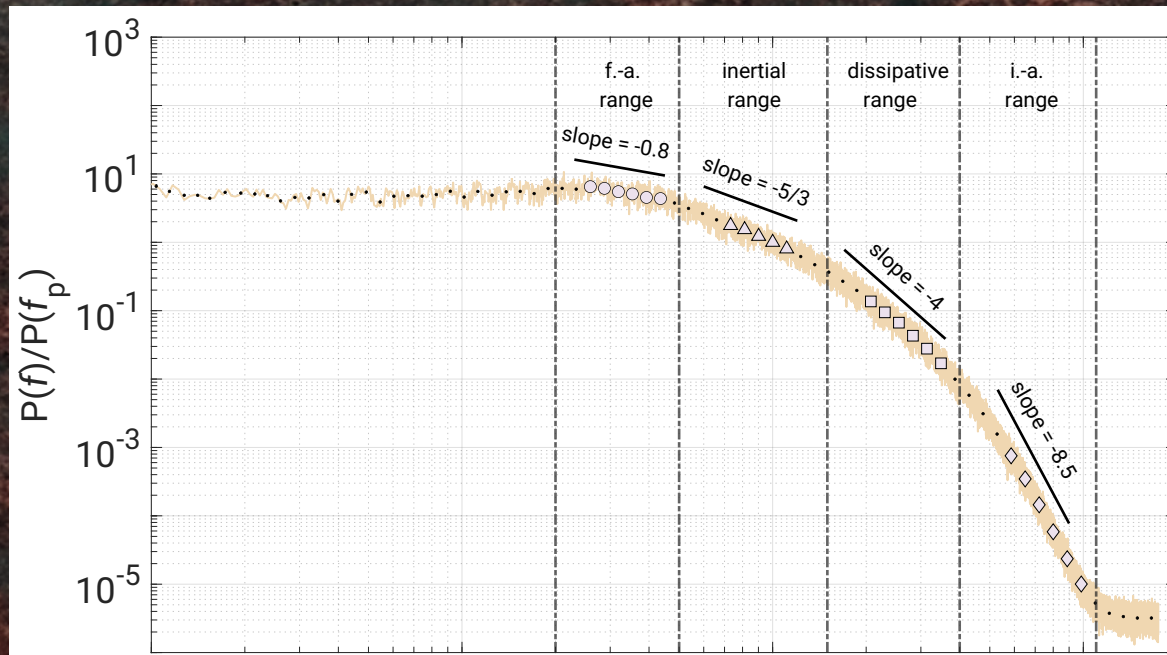
- scaling method proposed by Zhou and Xia (2001) – $f^2 P(f)$ – to collapse the PSD curves



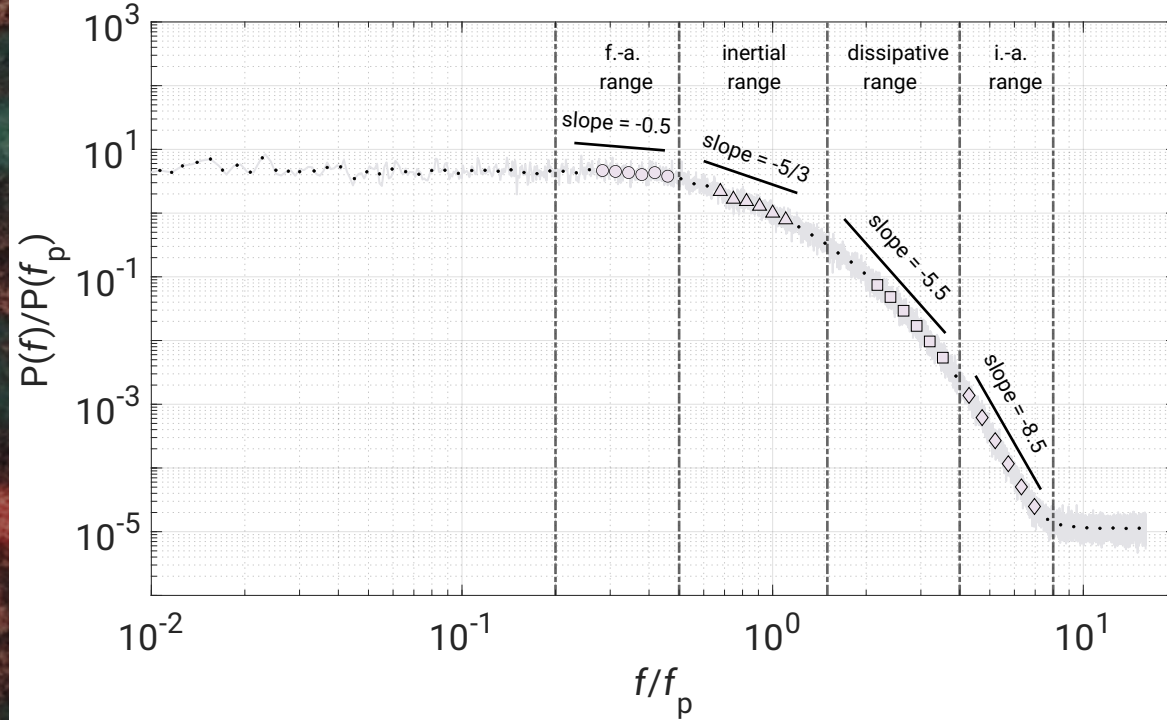
Power Spectral Density – regimes

Four defined regimes:

- facility-affected range
- inertial range
- dissipative range
- instrument-affected range



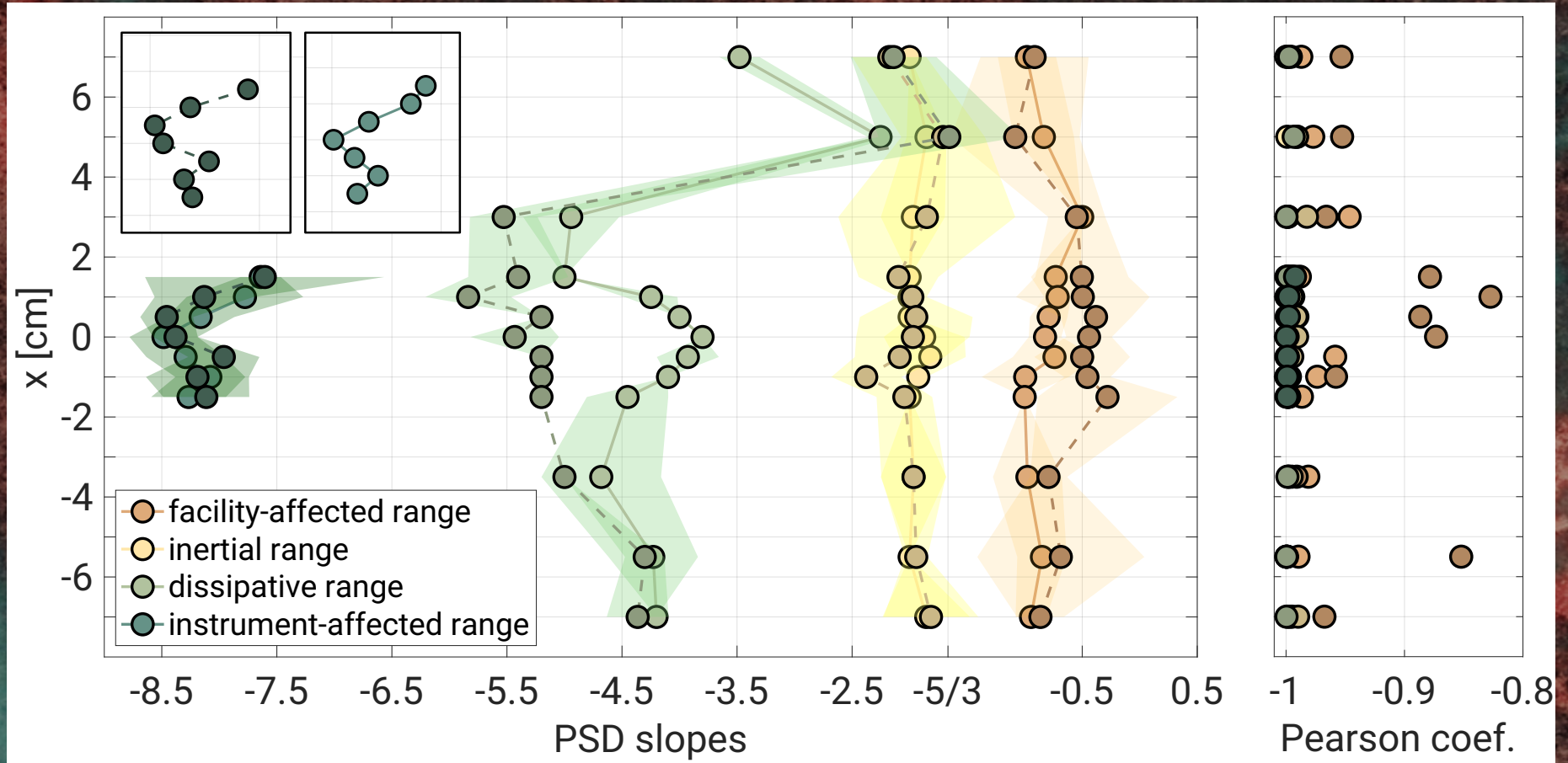
D-1-MIX



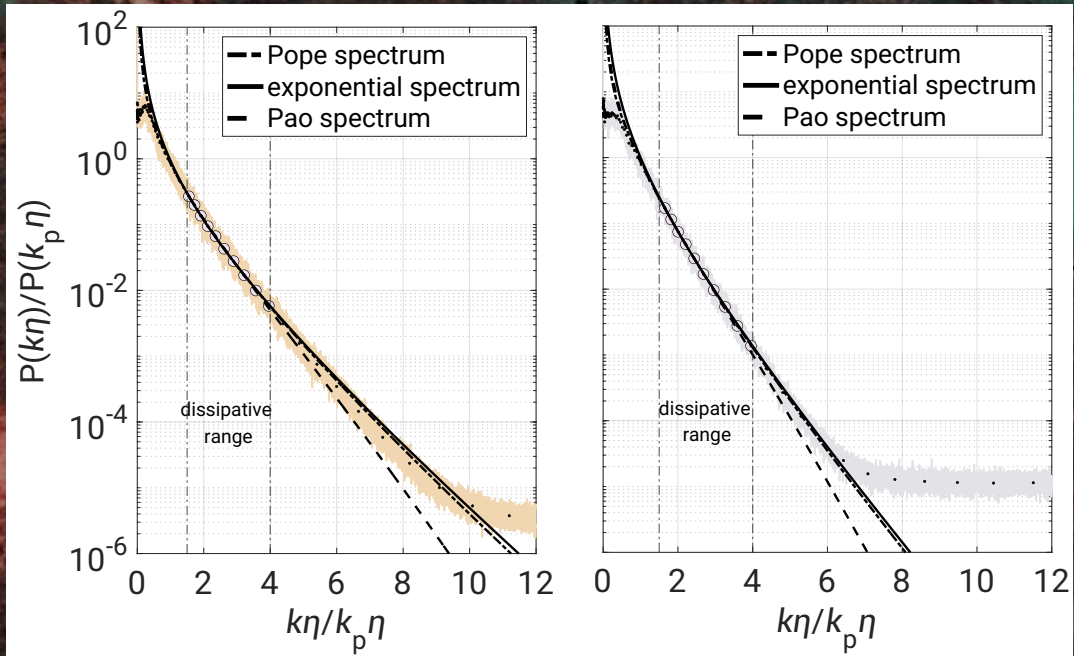
$x = 0$ cm

D-2-MIX

Power Spectral Density – slopes



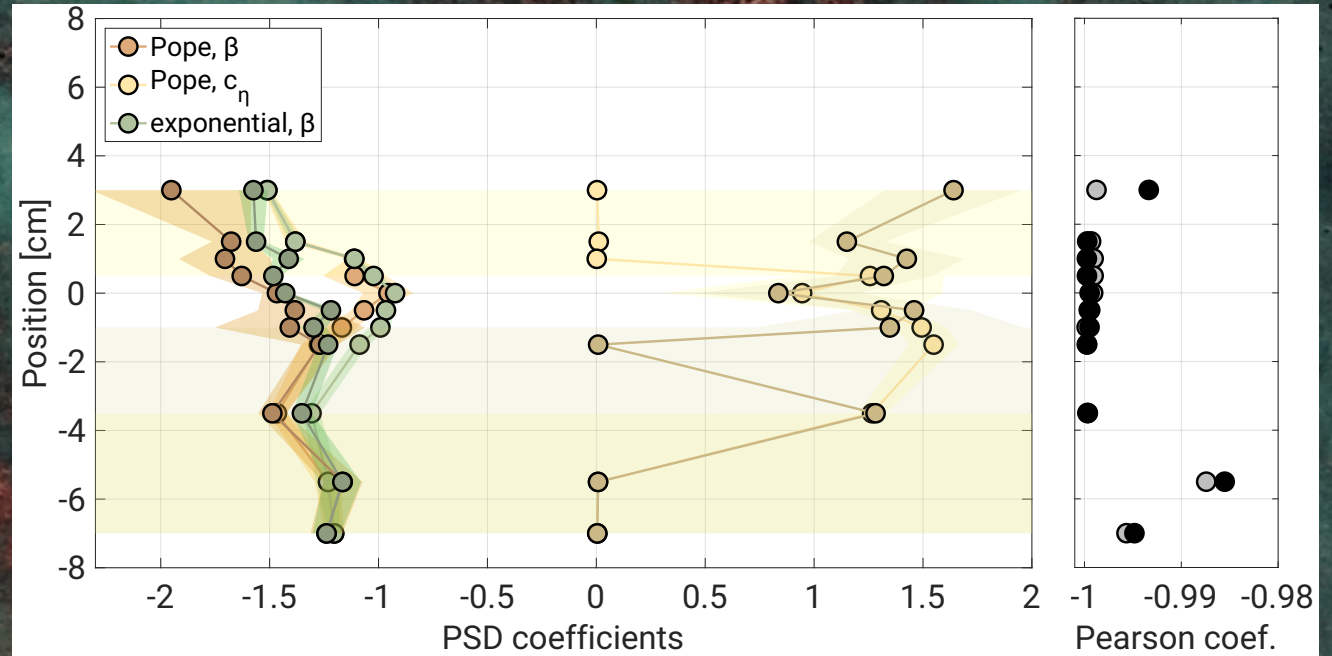
Power Spectral Density in wavenumber picture



D-1-MIX

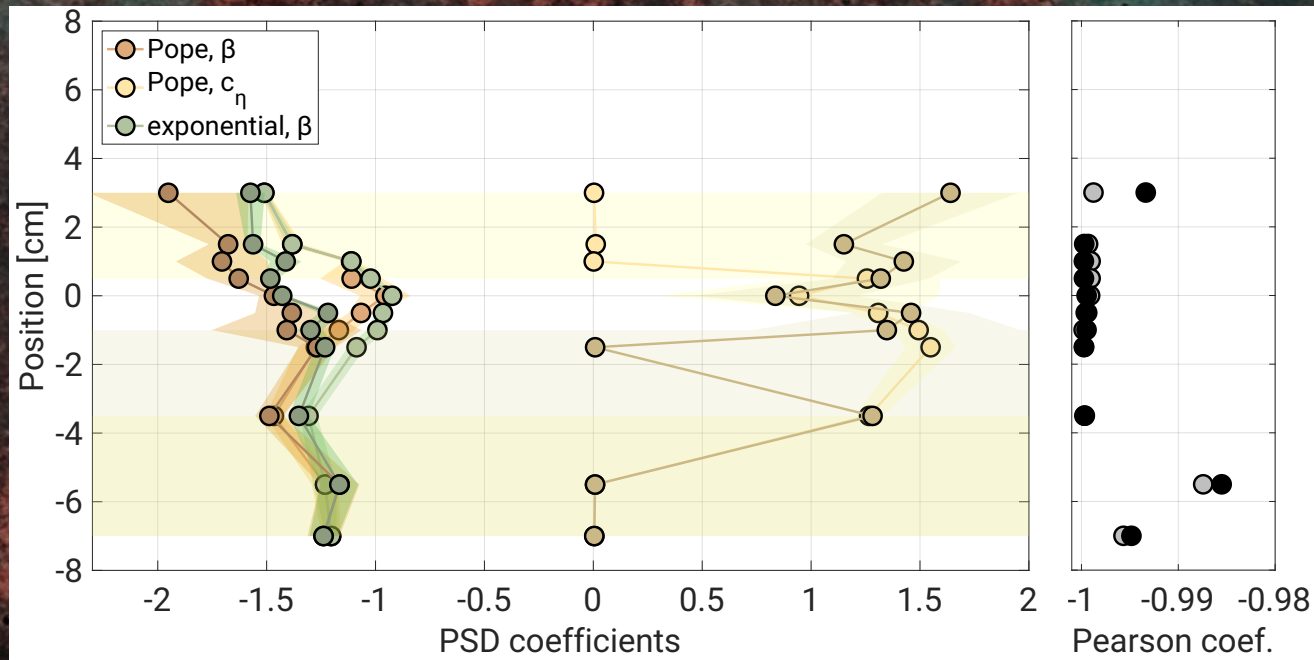
D-2-MIX

$x = 0$ cm

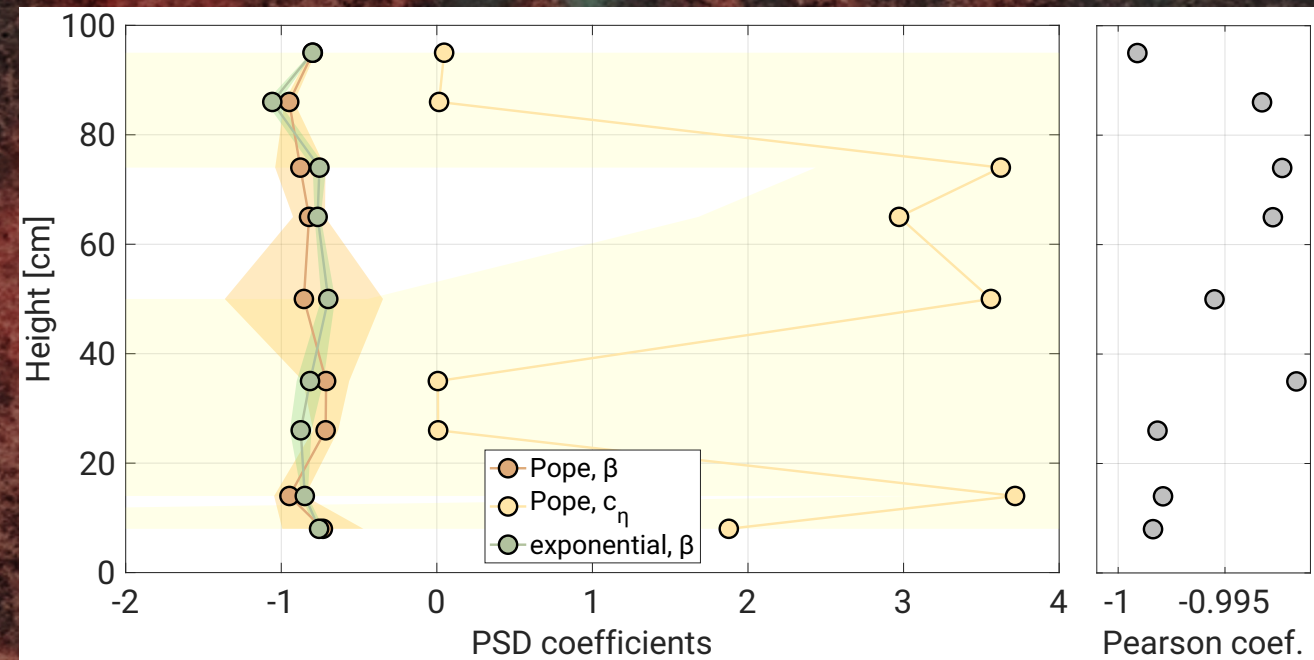


lighter color shades – D-1-MIX
darker color shades – D-2-MIX

Power Spectral Density – slopes



LACIS-T



Pi Chamber

II part-take away

- basic characteristics – standard deviation peaks shift attributed to differences in mixing dynamics between both cases; strong skewness inhomogeneity present on the right side of the tunnel -> likely due to obstacle presence; outside conditions affect regions near the windows;
- dynamic regimes – PSD analysis showed changing intensity of power spectra across the tunnel; four distinct power-law dynamic regimes were identified: facility-affected (~ -0.5 or ~ -0.8), inertial ($\sim -5/3$), dissipative (~ -4 or ~ -5.5), and instrument-affected (~ -8.5); the following dissipative regime analyses confirmed usability of analytical approach for the scalar spectrum showing that in the smallest scales LACIS-T results are consistent with the previous findings from the Pi Chamber;